A MIXED DISCONTINUOUS GALERKIN METHOD FOR INCOMPRESSIBLE MAGNETOHYDRODYNAMICS

PAUL HOUSTON *, DOMINIK SCHÖTZAU †, AND XIAOXI WEI ‡

Abstract. We introduce and analyze a discontinuous Galerkin method for the numerical discretization of a stationary incompressible magnetohydrodynamics model problem. The fluid unknowns are discretized with inf-sup stable discontinuous $\mathcal{P}_k^3 - \mathcal{P}_{k-1}$ elements whereas the magnetic part of the equations is approximated by discontinuous $\mathcal{P}_k^3 - \mathcal{P}_{k+1}$ elements. We carry out a complete a-priori error analysis and prove that the energy norm error is convergent of order $\mathcal{O}(h^k)$ in the mesh size h. We also show that the method is able to correctly capture and resolve the strongest magnetic singularities in non-convex polyhedral domains. These results are verified in a series of numerical experiments.

Key words. Incompressible magnetohydrodynamics, mixed finite element methods, discontinuous Galerkin methods

1. Introduction. Incompressible magnetohydrodynamics (MHD) models the interaction of viscous, electrically conducting incompressible fluids with electromagnetic fields. It has a number of technological and industrial applications such as metallurgical engineering, electromagnetic pumping, stirring of liquid metals, and measuring flow quantities based on magnetic induction; cf. [15, 20].

The numerical simulation of incompressible MHD problems requires discretizing a system of partial differential equations that couples the incompressible Navier-Stokes equations with Maxwell's equations. Various finite element methods (FEM) can be found in the literature where the magnetic field is approximated by standard nodal (i.e., H^1-conforming) finite elements, see, e.g., [2, 19, 22, 23] and the references therein. However, in non-convex polyhedra of engineering interest, the magnetic field may have regularity below H^1 and a nodal FEM discretization, albeit stable, can converge to a magnetic field that misses certain singular solution components induced by reentrant vertices or edges; see [14]. In the recent work [35], this drawback of nodal elements was overcome by the use of Nédélec elements for the approximation of the magnetic field. Thereby, a new variational setting for the formulation of incompressible MHD problems was proposed. This framework is based on a mixed approach for the discretization of the Maxwell operator and introduces a Lagrange multiplier related to the divergence constraint of the magnetic field, cf. [26, 32].

Over the last two decades, discontinuous Galerkin (DG) methods have become an integral part of computational fluid mechanics and computational electromagnetics, see [11, 12, 13, 17, 25] and the references therein. DG methods are extremely versatile and flexible; they can deal robustly with partial differential equations of almost any kind, as well as with equations whose type changes within the computational domain. Their intrinsic stability properties make them naturally suited for problems where convection is dominant. Moreover, discontinuous Galerkin methods can easily handle irregularly refined meshes and variable approximation degrees (*hp*-adaptivity). The

*School of Mathematical Sciences, University of Nottingham, University Park, Nottingham NG7 2RD, UK, E-mail: Paul.Houston@nottingham.ac.uk.

†Department of Mathematics, University of British Columbia, Vancouver, BC, V6T 1Z2, Canada. E-mail: schoetzau@math.ubc.ca. The work of the this author was partially supported by the National Sciences and Engineering Council of Canada (NSERC).

‡Department of Mathematics, University of British Columbia, Vancouver, BC, V6T 1Z2, Canada. E-mail: weixiaoxi@math.ubc.ca. The work of the this author was partially supported by the National Sciences and Engineering Council of Canada (NSERC).

DG approximations of magnetic or electric fields can be based on standard polynomial shape functions, in contrast to curl-conforming or divergence-conforming elements commonly used in computational electromagnetics. DG methods have already been successfully applied to both ideal and viscous compressible MHD problems [31, 37].

In this paper, we propose and analyze an interior penalty discontinuous Galerkin method for a linearized incompressible MHD model problem based on the mixed formulation introduced in [35]. Our method roots in the DG discretizations that have been developed recently for incompressible flow problems and Maxwell's equations. More specifically, the fluid unknowns are approximated using mixed discontinuous $\mathcal{P}_k^3 - \mathcal{P}_{k-1}$ elements [8, 9, 36] while the magnetic variables are discretized with the $\mathcal{P}_k^3 - \mathcal{P}_{k+1}$ element pair proposed and analyzed in [28, 29], see also [27]. We carry out a complete a-priori error analysis for the proposed DG method, and show that the energy error in the velocity and the L^2-norm error in the pressure are optimally convergent of order $\mathcal{O}(h^k)$ in the mesh size h. Moreover, the energy errors in the magnetic field and the magnetic multiplier are proven to converge with the order $\mathcal{O}(h^k)$ as well. While this order is optimal for the magnetic field, it is slightly suboptimal for the error in the multiplier. This is due to the fact that polynomials of degree $k+1$ are used for the approximation of the magnetic multiplier. The same suboptimality phenomenon is observed when using the second family Nédélec element pair [32]. On the other hand, the use of polynomials of degree $k+1$ in the approximation of the magnetic multiplier ensures optimality of the L^2-norm error of the magnetic field [27, 28]. Our results also show that the proposed DG method is able to correctly resolve the strongest magnetic singularities in non-convex polyhedral domains, in contrast to nodal elements that are often used for the approximation of the magnetic field.

The rest of the paper is organized as follows. In Section 2, we begin by introducing an interior penalty discontinuous Galerkin finite element method for the discretization of an incompressible MHD model problem. In Section 3, our main results are stated and discussed: a-priori error estimates for the method under consideration. Section 4 is devoted to the detailed proof of these results. In Section 5, we present a series of numerical experiments validating our theoretical results. Finally, we present some concluding remarks in Section 6.

2. Discontinuous Galerkin discretization of a model problem. In this section, we formulate a linearized MHD model problem and present its weak formulation. Then we discretize it using an interior penalty discontinuous Galerkin finite element method.

2.1. An MHD model problem. We consider the following linear and stationary MHD system based on the mixed formulation proposed in [35]: find the velocity field $\mathbf{u}$, the pressure p, the magnetic field $\mathbf{b}$, and the scalar potential r such that

$$-\nu\,\Delta\mathbf{u} + (\mathbf{w}\cdot\nabla)\mathbf{u} + \gamma\mathbf{u} + \nabla p - \kappa\,(\nabla\times\mathbf{b})\times\mathbf{d} = \mathbf{f} \qquad \text{in } \Omega, \tag{2.1}$$

$$\kappa\,\nu_m\,\nabla\times(\nabla\times\mathbf{b}) + \nabla r - \kappa\,\nabla\times(\mathbf{u}\times\mathbf{d}) = \mathbf{g} \qquad \text{in } \Omega, \tag{2.2}$$

$$\nabla\cdot\mathbf{u} = 0 \qquad \text{in } \Omega, \tag{2.3}$$

$$\nabla\cdot\mathbf{b} = 0 \qquad \text{in } \Omega. \tag{2.4}$$

Here, we take Ω to be a Lipschitz polyhedron in $\mathbb{R}^3$. We assume that Ω is simply-connected, and that its boundary Γ is connected. The function $\mathbf{w} \in L^\infty(\Omega)^3$ is a prescribed convective field with $\nabla\cdot\mathbf{w} \in L^\infty(\Omega)^3$, and $\mathbf{d} \in L^\infty(\Omega)^3$ is a given

magnetic field. Typically these fields come from a linearization process. The right-hand sides $\mathbf{f}$ and $\mathbf{g}$ are vector-valued source terms in $L^2(\Omega)^3$. The scalar function γ belongs to $L^\infty(\Omega)$. We further assume that there is a positive constant $\gamma_\star$ such that

$$\gamma_0(\mathbf{x}) := \gamma(\mathbf{x}) - \frac{1}{2}\nabla \cdot \mathbf{w}(\mathbf{x}) \geq \gamma_\star > 0, \qquad \mathbf{x} \in \Omega. \tag{2.5}$$

Without loss of generality, we may assume that the size of Ω, and the magnitudes of $\mathbf{w}$ and $\mathbf{d}$ are of order one. Then the equations contain three characteristic parameters: The quantity ν^{-1} is the hydrodynamic Reynolds number Re which represents the ratio of inertial forces to viscous forces. The second parameter ν_m^{-1} is the magnetic Reynolds number Rm. It measures how much the magnetic field will be influenced by the flow motion. The third parameter κ is the coupling number. The coupling number κ is typically expressed as a function of the so-called Hartmann number Ha:

$$\kappa = \nu\nu_m \mathrm{Ha}^2. \tag{2.6}$$

The parameter Ha is a measure of the ratio of electromagnetic forces to viscous forces.

REMARK 2.1. *In this paper, we will focus on the case where the magnitudes of* Rm *and* κ *are of order one, whereas* Re *can be substantially larger, as is the case in many engineering applications. For example, in aluminum electrolysis,* Re *is around* 10^5*, while the values of* Rm *and* κ *are in the range of* 10^{-1} *and 1, respectively. We refer the reader to [2] and [4] for the orders of magnitude of these parameters in other cases. For simplicity, we will thus not make explicit our error estimates with respect to* ν_m *and* κ*.*

We suppose that the boundary Γ of Ω can be partitioned into two disjoint parts. That is, we have $\overline{\Gamma} = \overline{\Gamma}_D \cup \overline{\Gamma}_N$ with $\Gamma_D \cap \Gamma_N = \emptyset$. Throughout, we assume that Γ_D is non-empty and satisfies $\int_{\Gamma_D} ds > 0$. We then supplement the MHD system (2.1)–(2.4) with the following boundary conditions:

$$\mathbf{u} = \mathbf{u}_D \qquad \text{on } \Gamma_D, \tag{2.7}$$

$$(p\underline{\mathrm{I}} - \nu\nabla\mathbf{u})\mathbf{n} = p_N\mathbf{n} \qquad \text{on } \Gamma_N, \tag{2.8}$$

$$\mathbf{n} \times \mathbf{b} = \mathbf{n} \times \mathbf{b}_D \qquad \text{on } \Gamma, \tag{2.9}$$

$$r = 0 \qquad \text{on } \Gamma. \tag{2.10}$$

Here, $\underline{\mathrm{I}}$ is the identity matrix in $\mathbb{R}^{3\times 3}$ and $\mathbf{n}$ is the unit outward normal vector on Γ. We assume that $p_N \in L^2(\Gamma_N)$. Moreover, we assume that the boundary data $\mathbf{u}_D$ and $\mathbf{b}_D$ can be extended to functions in Ω, also denoted by $\mathbf{u}_D$ and $\mathbf{b}_D$, so that

$$\mathbf{u}_D \in H^1(\Omega)^3 \cap H(\mathrm{div}^0;\Omega), \qquad \mathbf{b}_D \in H(\mathrm{curl};\Omega) \cap H(\mathrm{div}^0;\Omega), \tag{2.11}$$

where

$$H(\mathrm{curl};\Omega) = \left\{ \mathbf{b} \in L^2(\Omega)^3 \,:\, \nabla \times \mathbf{b} \in L^2(\Omega)^3 \right\},$$
$$H(\mathrm{div}^0;\Omega) = \left\{ \mathbf{b} \in L^2(\Omega)^3 \,:\, \nabla \cdot \mathbf{b} = 0 \text{ in } \Omega \right\}.$$

For the velocity datum $\mathbf{u}_D$, a lifting of this type has been constructed in [21, Lemma IV.2.3] (when $\Gamma_N = \emptyset$). For the lifting of $\mathbf{b}_D$, we refer to [34, Proposition A.1]. Finally, we notice that, if $\Gamma_N = \emptyset$, the datum $\mathbf{u}_D$ must satisfy the compatibility condition $\int_\Gamma \mathbf{u}_D \cdot \mathbf{n}\, ds = 0$.

We also define the inflow and outflow boundaries of Ω as

$$\Gamma_- = \{\, \mathbf{x} \in \Gamma : \mathbf{w}(\mathbf{x}) \cdot \mathbf{n}(\mathbf{x}) < 0 \,\} \quad \text{and} \quad \Gamma_+ = \{\, \mathbf{x} \in \Gamma : \mathbf{w}(\mathbf{x}) \cdot \mathbf{n}(\mathbf{x}) \geq 0 \,\},$$

respectively. We adopt the (physically reasonable) hypothesis that

$$\mathbf{w}(\mathbf{x}) \cdot \mathbf{n}(\mathbf{x}) \geq 0 \quad \text{for all } \mathbf{x} \in \Gamma_N. \tag{2.12}$$

Obviously, we then have $\Gamma_- \subseteq \Gamma_D$.

REMARK 2.2. *We point out that the MHD system (2.1)–(2.4) is a linearized version of the fully non-linear stationary MHD system studied in [35]. Indeed, using a Picard-type iteration procedure for the non-linear equations in [35] yields a linear problem of the form (2.1)–(2.4) in each iteration step.*

As in [35], we use a mixed approach to discretize the Maxwell operator; see also [26, 32]. This has the advantage that the strongest magnetic singularities can be correctly captured and resolved in non-convex domains, in contrast to classical approaches that employ nodal elements and regularization of the electrostatic equation (2.2). The scalar potential r is the Lagrange multiplier associated with this mixed formulation. By taking the divergence of (2.2), we see that

$$-\Delta r = \nabla \cdot \mathbf{g} \quad \textit{in} \quad \Omega, \qquad r = 0 \quad \textit{on} \quad \Gamma. \tag{2.13}$$

In particular, we have $r = 0$ provided that the function $\mathbf{g}$ is divergence-free. In this case, the MHD problem (2.1)–(2.4) is the same as the linearized version of the one considered in [23] or the one studied in [19].

2.2. Weak formulation. On introducing the Sobolev spaces

$$\begin{aligned}
\mathbf{V} &= \left\{\, \mathbf{u} \in H^1(\Omega)^3 \,:\, \mathbf{u} = 0 \text{ on } \Gamma_D \,\right\}, \\
\mathbf{C} &= \{\, \mathbf{b} \in H(\mathrm{curl};\Omega) \,:\, \mathbf{n} \times \mathbf{b} = \mathbf{0} \text{ on } \Gamma \,\}, \\
S &= H_0^1(\Omega),
\end{aligned}$$

and the pressure space

$$Q = \begin{cases} L_0^2(\Omega) = \{\, u \in L^2(\Omega) \,:\, (u,1)_\Omega = 0 \,\} & \text{if } \Gamma_N = \emptyset, \\ L^2(\Omega) & \text{otherwise,} \end{cases}$$

the weak formulation of the incompressible MHD system (2.1)–(2.4) consists in finding $(\mathbf{u}, \mathbf{b}, p, r) \in H^1(\Omega)^3 \times H(\mathrm{curl};\Omega) \times Q \times S$, with $\mathbf{u} = \mathbf{u}_D$ on Γ_D and $\mathbf{n} \times \mathbf{b} = \mathbf{n} \times \mathbf{b}_D$ on Γ, such that

$$A(\mathbf{u},\mathbf{v}) + O(\mathbf{u},\mathbf{v}) + C(\mathbf{v},\mathbf{b}) + B(\mathbf{v},p) = (\mathbf{f},\mathbf{v})_\Omega - \langle p_N \mathbf{n}, \mathbf{v} \rangle_{\Gamma_N}, \tag{2.14}$$

$$M(\mathbf{b},\mathbf{c}) - C(\mathbf{u},\mathbf{c}) + D(\mathbf{c},r) = (\mathbf{g},\mathbf{c})_\Omega, \tag{2.15}$$

$$B(\mathbf{u},q) = 0, \tag{2.16}$$

$$D(\mathbf{b},s) = 0, \tag{2.17}$$

for all $(\mathbf{v}, \mathbf{c}, q, s) \in \mathbf{V} \times \mathbf{C} \times Q \times S$. Here, the bilinear forms are given by

$$\begin{aligned} A(\mathbf{u}, \mathbf{v}) &= \int_\Omega \nu \nabla \mathbf{u} : \nabla \mathbf{v} \, d\mathbf{x}, \\ O(\mathbf{u}, \mathbf{v}) &= \int_\Omega (\,(\mathbf{w} \cdot \nabla)\mathbf{u} + \gamma\, \mathbf{u}) \cdot \mathbf{v} \, d\mathbf{x}, \\ M(\mathbf{b}, \mathbf{c}) &= \int_\Omega \kappa\, \nu_m (\nabla \times \mathbf{b}) \cdot (\nabla \times \mathbf{c}) \, d\mathbf{x}, \\ C(\mathbf{v}, \mathbf{b}) &= \int_\Omega \kappa\, (\mathbf{v} \times \mathbf{d}) \cdot (\nabla \times \mathbf{b}) \, d\mathbf{x}, \\ B(\mathbf{u}, q) &= -\int_\Omega (\nabla \cdot \mathbf{u})\, q \, d\mathbf{x}, \\ D(\mathbf{b}, s) &= \int_\Omega \mathbf{b} \cdot \nabla s \, d\mathbf{x}. \end{aligned} \tag{2.18}$$

The well-posedness of this problem follows from the theory of mixed finite elements [6] and well-known stability properties, taking into account assumptions (2.5), (2.11) and (2.12). We also refer to [35] for the well-posedness of a closely related non-linear incompressible MHD problem.

2.3. Discretization. We now introduce a discontinuous Galerkin discretization for the incompressible MHD problem (2.1)–(2.4).

2.3.1. Meshes and finite element spaces. We consider a family of regular and shape-regular triangulations $\mathcal{T}_h$ that partition the domain Ω into tetrahedra $\{K\}$. We denote by $\mathcal{F}_h^I$ the set of all interior faces of $\mathcal{T}_h$, and by $\mathcal{F}_h^B$ the set of all boundary faces. We always assume that $\mathcal{F}_h^B$ can be divided into two disjoint sets $\mathcal{F}_h^D$ and $\mathcal{F}_h^N$ of Dirichlet and Neumann faces, respectively. That is, we assume that $\mathcal{F}_h^B = \mathcal{F}_h^D \cup \mathcal{F}_h^N$ where

$$\overline{\Gamma}_D = \cup_{F \in \mathcal{F}_h^D} \overline{F}, \qquad \overline{\Gamma}_N = \cup_{F \in \mathcal{F}_h^N} \overline{F}. \tag{2.19}$$

As usual, h_K denotes the diameter of the element K, and h_F is the diameter of the face F. The mesh size of $\mathcal{T}_h$ is given by $h = \max_{K \in \mathcal{T}_h} h_K$. Finally, we write $\mathbf{n}_K$ to denote the outward unit normal vector on the boundary ∂K of the element K.

Next, we introduce the average and jump operators. To do so, let $F = \partial K \cap \partial K'$ be an interior face shared by K and K' and let $\mathbf{x} \in F$. Let φ be a generic piecewise smooth function and denote by φ and φ' the traces of φ on F taken from within the interior of K and K', respectively. Then, we define the mean value $\{\!\{\cdot\}\!\}$ at $\mathbf{x} \in F$ as

$$\{\!\{\varphi\}\!\} = \frac{1}{2}(\varphi + \varphi').$$

Furthermore, for a piecewise smooth scalar function u, we define the (vector-valued) jump $[\![\cdot]\!]$ at $\mathbf{x} \in F$ as

$$[\![u]\!] = u\, \mathbf{n}_K + u'\, \mathbf{n}_{K'}.$$

Similarly, if $\mathbf{u}$ is a piecewise smooth vector-valued function, we define the following three types of jumps:

$$[\![\mathbf{u}]\!] = \mathbf{u} \otimes \mathbf{n}_K + \mathbf{u}' \otimes \mathbf{n}_{K'}, \quad [\![\mathbf{u}]\!]_T = \mathbf{n}_K \times \mathbf{u} + \mathbf{n}_{K'} \times \mathbf{u}', \quad [\![\mathbf{u}]\!]_N = \mathbf{u} \cdot \mathbf{n}_K + \mathbf{u}' \cdot \mathbf{n}_{K'},$$

where $\mathbf{u} \otimes \mathbf{n} = (u_i n_j)_{1 \le i,j \le 3}$. Note that $[\![\mathbf{u}]\!]_T$ and $[\![\mathbf{u}]\!]_N$ denote the tangential and normal jumps, respectively, whereas $[\![\mathbf{u}]\!]$ is the full jump in all the components of the vector field $\mathbf{u}$. On a boundary face $F = \partial K \cap \Gamma$, we set accordingly

$$\{\!\{\varphi\}\!\} = \varphi, \quad [\![u]\!] = u\,\mathbf{n}, \quad [\![\mathbf{u}]\!] = \mathbf{u} \otimes \mathbf{n}, \quad [\![\mathbf{u}]\!]_T = \mathbf{n} \times \mathbf{u}, \quad [\![\mathbf{u}]\!]_N = \mathbf{u} \cdot \mathbf{n}.$$

Here, we recall that $\mathbf{n}$ is the unit outward normal on the boundary Γ.

For $k \ge 1$, we now wish to approximate the solution $(\mathbf{u}, \mathbf{b}, p, r)$ of the MHD problem (2.1)–(2.4) by finite element functions $(\mathbf{u}_h, \mathbf{b}_h, p_h, r_h) \in \mathbf{V}_h \times \mathbf{C}_h \times Q_h \times S_h$, where

$$\begin{aligned} \mathbf{V}_h &= \left\{ \mathbf{u} \in L^2(\Omega)^3 \,:\, \mathbf{u}|_K \in \mathcal{P}_k(K)^3,\, K \in \mathcal{T}_h \right\}, \\ \mathbf{C}_h &= \left\{ \mathbf{b} \in L^2(\Omega)^3 \,:\, \mathbf{b}|_K \in \mathcal{P}_k(K)^3,\, K \in \mathcal{T}_h \right\}, \\ Q_h &= \left\{ p \in Q \,:\, p|_K \in \mathcal{P}_{k-1}(K),\, K \in \mathcal{T}_h \right\}, \\ S_h &= \left\{ r \in L^2(\Omega) \,:\, r|_K \in \mathcal{P}_{k+1}(K),\, K \in \mathcal{T}_h \right\}, \end{aligned} \tag{2.20}$$

with $\mathcal{P}_k(K)$ denoting the polynomials of total degree at most k on K.

2.3.2. Interior penalty formulation. We consider the following discontinuous Galerkin method: find $(\mathbf{u}_h, \mathbf{b}_h, p_h, r_h) \in \mathbf{V}_h \times \mathbf{C}_h \times Q_h \times S_h$ such that

$$A_h(\mathbf{u}_h, \mathbf{v}) + O_h(\mathbf{u}_h, \mathbf{v}) + C_h(\mathbf{v}, \mathbf{b}_h) + B_h(\mathbf{v}, p_h) = F_h(\mathbf{v}), \tag{2.21}$$

$$M_h(\mathbf{b}_h, \mathbf{c}) - C_h(\mathbf{u}_h, \mathbf{c}) + D_h(\mathbf{c}, r_h) = G_h(\mathbf{c}), \tag{2.22}$$

$$B_h(\mathbf{u}_h, q) = \langle \mathbf{u}_D \cdot \mathbf{n}, q \rangle_{\Gamma_D}, \tag{2.23}$$

$$D_h(\mathbf{b}_h, s) - J_h(r_h, s) = 0 \tag{2.24}$$

for all $(\mathbf{v}, \mathbf{c}, q, s) \in \mathbf{V}_h \times \mathbf{C}_h \times Q_h \times S_h$.

Here, the forms related to the discretization of the Oseen operator are the ones proposed and studied in [8, 9, 24, 36]. The form A_h associated with the Laplacian is chosen to be the standard interior penalty form:

$$\begin{aligned} A_h(\mathbf{u}, \mathbf{v}) = &\sum_{K \in \mathcal{T}_h} \int_K \nu\, \nabla \mathbf{u} : \nabla \mathbf{v}\, d\mathbf{x} - \sum_{F \in \mathcal{F}_h^I \cup \mathcal{F}_h^D} \int_F \{\!\{\nu \nabla \mathbf{u}\}\!\} : [\![\mathbf{v}]\!]\, ds \\ &- \sum_{F \in \mathcal{F}_h^I \cup \mathcal{F}_h^D} \int_F \{\!\{\nu \nabla \mathbf{v}\}\!\} : [\![\mathbf{u}]\!]\, ds + \sum_{F \in \mathcal{F}_h^I \cup \mathcal{F}_h^D} \frac{\nu a_0}{h_F} \int_F [\![\mathbf{u}]\!] : [\![\mathbf{v}]\!]\, ds. \end{aligned} \tag{2.25}$$

The parameter $a_0 > 0$ is a stabilization parameter; it has to be chosen larger than a threshold value which is independent of the mesh size and ν, ν_m and κ, see Proposition 3.1 below. For the convective form, we take the usual upwind form defined by

$$\begin{aligned} O_h(\mathbf{u}, \mathbf{v}) = &\sum_{K \in \mathcal{T}_h} \int_K ((\mathbf{w} \cdot \nabla)\mathbf{u} + \gamma\, \mathbf{u}) \cdot \mathbf{v}\, d\mathbf{x} \\ &+ \sum_{K \in \mathcal{T}_h} \int_{\partial K_- \setminus \Gamma_-} \mathbf{w} \cdot \mathbf{n}_K (\mathbf{u}^e - \mathbf{u}) \cdot \mathbf{v}\, ds - \int_{\Gamma_-} \mathbf{w} \cdot \mathbf{n} \mathbf{u} \cdot \mathbf{v}\, ds. \end{aligned} \tag{2.26}$$

Here, we denote by $\mathbf{u}^e$ the value of the trace of $\mathbf{u}$ taken from the exterior of element K. Moreover, we set ∂K_- and ∂K_+ to be the inflow and outflow boundaries of K, respectively, with respect to $\mathbf{w}$. They are defined by

$$\partial K_- = \{\, \mathbf{x} \in \partial K \,:\, \mathbf{w}(\mathbf{x}) \cdot \mathbf{n}_K(\mathbf{x}) < 0 \,\}, \quad \partial K_+ = \{\, \mathbf{x} \in \partial K \,:\, \mathbf{w}(\mathbf{x}) \cdot \mathbf{n}_K \geq 0 \,\}.$$

Upon integration by parts, the form O_h can be written as

$$\begin{aligned} O_h(\mathbf{u}, \mathbf{v}) = &- \sum_{K \in \mathcal{T}_h} \int_K (\mathbf{w} \cdot \nabla)\mathbf{v} \cdot \mathbf{u} \, d\mathbf{x} + \sum_{K \in \mathcal{T}_h} \int_K (\gamma - \nabla \cdot \mathbf{w})\mathbf{u} \cdot \mathbf{v} \, d\mathbf{x} \\ &+ \sum_{K \in \mathcal{T}_h} \int_{\partial K_+ \setminus \Gamma_+} \mathbf{w} \cdot \mathbf{n}_K \mathbf{u} \cdot (\mathbf{v} - \mathbf{v}^e) \, ds + \int_{\Gamma_+} \mathbf{w} \cdot \mathbf{n}\mathbf{u} \cdot \mathbf{v} \, ds. \end{aligned} \tag{2.27}$$

The form B_h related to the divergence constraint $-\nabla \cdot \mathbf{u} = 0$ is defined by

$$B_h(\mathbf{u}, q) = - \sum_{K \in \mathcal{T}_h} \int_K (\nabla \cdot \mathbf{u}) \, q \, d\mathbf{x} + \sum_{F \in \mathcal{F}_h^I \cup \mathcal{F}_h^D} \int_F \{\!\{q\}\!\} [\![\mathbf{u}]\!]_N \, ds. \tag{2.28}$$

Next, we introduce the forms for the discretization of the Maxwell operator. Our choice corresponds to the non-stabilized $\mathcal{P}_k^3 - \mathcal{P}_{k+1}$ interior penalty methods proposed and analyzed in [28, 29]. The form M_h related to the curl-curl operator is given by

$$\begin{aligned} M_h(\mathbf{b}, \mathbf{c}) = &\sum_{K \in \mathcal{T}_h} \int_K \kappa \, \nu_m (\nabla \times \mathbf{b}) \cdot (\nabla \times \mathbf{c}) \, d\mathbf{x} - \sum_{F \in \mathcal{F}_h} \int_F \{\!\{\kappa \nu_m \nabla \times \mathbf{b}\}\!\} \cdot [\![\mathbf{c}]\!]_T \, ds \\ &- \sum_{F \in \mathcal{F}_h} \int_F \{\!\{\kappa \nu_m \nabla \times \mathbf{c}\}\!\} \cdot [\![\mathbf{b}]\!]_T \, ds + \sum_{F \in \mathcal{F}_h} \kappa \nu_m \frac{m_0}{h_F} \int_F [\![\mathbf{b}]\!]_T \cdot [\![\mathbf{c}]\!]_T \, ds. \end{aligned} \tag{2.29}$$

The last term in M_h penalizes the tangential jump of the magnetic field. As for the diffusion form, to ensure stability, the stabilization parameter $m_0 > 0$ must be chosen large enough, independently of the mesh size and the parameters ν, ν_m, and κ, see Proposition 3.1 below.

The form D_h associated with the constraint $-\nabla \cdot \mathbf{b} = 0$ is defined by

$$D_h(\mathbf{b}, s) = \sum_{K \in \mathcal{T}_h} \int_K \mathbf{b} \cdot \nabla s \, d\mathbf{x} - \sum_{F \in \mathcal{F}_h} \int_F \{\!\{\mathbf{b}\}\!\} \cdot [\![s]\!] \, ds. \tag{2.30}$$

The form J_h is a stabilization term that ensures the H^1-conformity of the multiplier r_h. It is given by

$$J_h(r, s) = \sum_{F \in \mathcal{F}_h} \frac{s_0}{\kappa \nu_m h_F} \int_F [\![r]\!] \cdot [\![s]\!] \, ds, \tag{2.31}$$

with $s_0 > 0$ denoting a positive stabilization parameter. The dependence on ν_m and κ is chosen so as to suitably balance the multiplier terms in our error analysis.

For the coupling form C_h in (2.21) and (2.22), we take a discontinuous Galerkin version of the bilinear form C defined in (2.18), namely,

$$C_h(\mathbf{v}, \mathbf{b}) = \sum_{K \in \mathcal{T}_h} \kappa \int_K (\mathbf{v} \times \mathbf{d}) \cdot (\nabla \times \mathbf{b}) \, d\mathbf{x} - \sum_{F \in \mathcal{F}_h^I \cup \mathcal{F}_h^N} \kappa \int_F \{\!\{\mathbf{v} \times \mathbf{d}\}\!\} \cdot [\![\mathbf{b}]\!]_T \, ds. \tag{2.32}$$

Finally, the source terms $F_h(\mathbf{v})$ and $G_h(\mathbf{c})$ are given, respectively, by

$$\begin{aligned} F_h(\mathbf{v}) = & \int_\Omega \mathbf{f}\cdot\mathbf{v}\,d\mathbf{x} - \sum_{F\in\mathcal{F}_h^D}\int_F \nu\nabla\mathbf{v} : (\mathbf{u}_D\otimes\mathbf{n})\,ds \\ & + \sum_{F\in\mathcal{F}_h^D}\frac{\nu a_0}{h_F}\int_F \mathbf{u}_D\cdot\mathbf{v}\,ds - \sum_{F\in\mathcal{F}_h^N}\int_F \kappa(\mathbf{v}\times\mathbf{d})\cdot(\mathbf{n}\times\mathbf{b}_D)\,ds \\ & - \int_{\Gamma_-}\mathbf{w}\cdot\mathbf{n}\mathbf{u}_D\cdot\mathbf{v}\,ds - \sum_{F\in\mathcal{F}_h^N}\int_F p_N\mathbf{n}\cdot\mathbf{v}\,ds, \end{aligned} \tag{2.33}$$

and

$$\begin{aligned} G_h(\mathbf{c}) = & \int_\Omega \mathbf{g}\cdot\mathbf{c}\,d\mathbf{x} - \sum_{F\in\mathcal{F}_h^B}\int_F \kappa\nu_m(\nabla\times\mathbf{c})\cdot(\mathbf{n}\times\mathbf{b}_D)\,ds \\ & + \sum_{F\in\mathcal{F}_h^B}\kappa\nu_m\frac{m_0}{h_F}\int_F (\mathbf{n}\times\mathbf{b}_D)\cdot(\mathbf{n}\times\mathbf{c})\,ds \\ & - \sum_{F\in\mathcal{F}_h^D}\int_F \kappa(\mathbf{u}_D\times\mathbf{d})\cdot(\mathbf{n}\times\mathbf{c})\,ds. \end{aligned} \tag{2.34}$$

3. Main results. In this section, we present the main results of this paper. First, we review the stability properties of the discontinuous Galerkin method proposed in (2.21)–(2.24), and show that it has a unique solution. Then, we state and discuss a-priori error estimates for the error measured in terms of a natural energy norm.

3.1. Stability. To discuss the stability properties of the discontinuous Galerkin forms used in (2.21)–(2.24), we introduce several semi-norms and norms.

First, for the hydrodynamic velocity, we define

$$\begin{aligned} |\mathbf{u}|_{V^\perp}^2 &= \sum_{F\in\mathcal{F}_h^I\cup\mathcal{F}_h^D} h_F^{-1}\|[\![\mathbf{u}]\!]\|_{L^2(F)}^2, \\ \|\mathbf{u}\|_{1,h}^2 &= \sum_{K\in\mathcal{T}_h}\|\nabla\mathbf{u}\|_{L^2(K)}^2 + |\mathbf{u}|_{V^\perp}^2, \\ \|\mathbf{u}\|_V^2 &= \nu\|\mathbf{u}\|_{1,h}^2 + \|\gamma_0^{\frac{1}{2}}\mathbf{u}\|_{L^2(\Omega)}^2 + \frac{1}{2}\sum_{F\in\mathcal{F}_h}\||\mathbf{w}\cdot\mathbf{n}|^{\frac{1}{2}}[\![\mathbf{u}]\!]\|_{L^2(F)}^2. \end{aligned}$$

In the last term in the definition of $\|\cdot\|_V$, the vector $\mathbf{n}$ is any unit normal vector on the face under consideration. For the pressure, we will use $\|p\|_Q^2 = \nu^{-1}\|p\|_{L^2(\Omega)}^2$.

For the magnetic variables, we define the following semi-norms and norm:

$$\begin{aligned} |\mathbf{b}|_{C^\perp}^2 &= \kappa\nu_m\sum_{F\in\mathcal{F}_h} h_F^{-1}\|[\![\mathbf{c}]\!]_T\|_{L^2(F)}^2, \\ |\mathbf{b}|_C^2 &= \kappa\nu_m\sum_{K\in\mathcal{T}_h}\|\nabla\times\mathbf{b}\|_{L^2(K)}^2 + |\mathbf{b}|_{C^\perp}^2, \\ \|\mathbf{b}\|_C^2 &= \kappa\nu_m\|\mathbf{b}\|_{L^2(\Omega)}^2 + |\mathbf{b}|_C^2. \end{aligned}$$

Finally, on the multiplier space, we introduce

$$|r|_S^2 = \kappa^{-1}\nu_m^{-1} \sum_{F\in\mathcal{F}_h} h_F^{-1}\|[\![r]\!]\|_{L^2(F)}^2,$$

$$\|r\|_S^2 = \kappa^{-1}\nu_m^{-1} \sum_{K\in\mathcal{T}_h} \|\nabla r\|_{L^2(K)}^2 + |r|_S^2.$$

Let us now recall some of the well-known stability properties for the discontinuous Galerkin forms involved. First, we state the following well-known coercivity properties, see [3, 8, 28] and the references therein.

PROPOSITION 3.1. *There holds:*

(i) Under assumption (2.5), there is a threshold value $\underline{a}_0 > 0$, independent of the mesh size, ν, ν_m and κ, such that for every $a_0 \geq \underline{a}_0$ there is constant $C > 0$ independent of the mesh size, ν, ν_m and κ such that

$$A_h(\mathbf{u},\mathbf{u}) + O_h(\mathbf{u},\mathbf{u}) \geq C\|\mathbf{u}\|_V^2, \qquad \mathbf{u}\in\mathbf{V}_h.$$

(ii) There is a threshold value $\underline{m}_0 > 0$, independent of the mesh size, ν, ν_m, and κ, such that for $m_0 \geq \underline{m}_0$ there is a constant $C > 0$ independent of the mesh size, ν, ν_m and κ such that $M_h(\mathbf{b},\mathbf{b}) \geq C|\mathbf{b}|_C^2$ holds for all $\mathbf{b}\in\mathbf{C}_h$.

Next, we point out that the velocity/pressure pair $\mathbf{V}_h \times Q_h$ is inf-sup stable; cf. [6, Remark II.2.10] and [24, Proposition 10].

PROPOSITION 3.2. *There is a stability constant $C > 0$ independent of the mesh size, ν, ν_m and κ such that*

$$\inf_{p\in Q_h} \sup_{\mathbf{u}\in\mathbf{V}_h} \frac{B_h(\mathbf{u},p)}{\|\mathbf{u}\|_{1,h}\|p\|_{L^2(\Omega)}} \geq C > 0.$$

There is no inf-sup condition available for the pair $\mathbf{C}_h \times S_h$. However, the underlying conforming spaces are stable, see [26, 32]. To discuss this, we introduce the conforming spaces $\mathbf{C}_h^c = \mathbf{C}_h \cap \mathbf{C}$ and $S_h^c = S_h \cap S$. The space $\mathbf{C}_h^c$ is the Nédélec finite element space of the second type of order k [32, 33], with zero tangential trace enforced on the boundary Γ. The space S_h^c is the space of continuous polynomials of degree $k+1$, with zero trace on Γ. Thus, we may decompose $\mathbf{C}_h$ and S_h into

$$\mathbf{C}_h = \mathbf{C}_h^c \oplus \mathbf{C}_h^\perp, \qquad S_h = S_h^c \oplus S_h^\perp, \tag{3.1}$$

respectively. Obviously, the semi-norms $|\cdot|_{C^\perp}$ and $|\cdot|_S$ define norms on $\mathbf{C}_h^\perp$ and $S_h^\perp$, respectively. The following norm-equivalence results from [28, Theorem 4.1] are essential to our error analysis.

PROPOSITION 3.3. *There is a constant $C > 0$, independent of the mesh size, ν,ν_m and κ, such that*

$$C\|\mathbf{b}\|_C \leq |\mathbf{b}|_{C^\perp} \leq \|\mathbf{b}\|_C, \qquad C\|r\|_S \leq |r|_S \leq \|r\|_S,$$

for any $\mathbf{b}\in\mathbf{C}_h^\perp$ and $r\in S_h^\perp$.

The conforming pair $\mathbf{C}_h^c \times S_h^c$ is stable and satisfies the following properties, see [28, Lemma 5.3] for a proof.

PROPOSITION 3.4. *There holds:*

(i) The bilinear form M is coercive on the conforming kernel of D in $\mathbf{C}_h^c$. That is, there exists a constant $C > 0$ independent of the mesh size, ν, ν_m and κ such that

$$M(\mathbf{b}, \mathbf{b}) \geq C\|\mathbf{b}\|_C^2,$$

for any $\mathbf{b}$ in $\mathbf{X}_h^c$, where

$$\mathbf{X}_h^c = \{\, \mathbf{b} \in \mathbf{C}_h^c \,:\, D(\mathbf{b}, s) = 0 \quad \forall\, s \in S_h^c \,\}. \tag{3.2}$$

(ii) The form D is inf-sup stable on $\mathbf{C}_h^c \times S_h^c$. That is, there exists a constant $C > 0$ independent of the mesh size, ν, ν_m and κ such that

$$\inf_{r \in S_h^c} \sup_{\mathbf{b} \in \mathbf{C}_h^c} \frac{D(\mathbf{b}, r)}{\|\mathbf{b}\|_C \|r\|_S} \geq C > 0.$$

In the spirit of [7], we will use the stability properties of the conforming spaces to derive error estimates for the magnetic variables. The non-conformity of the DG method will then be controlled by using the norm-equivalence estimates in Proposition 3.3.

We are now ready to prove that the DG formulation is uniquely solvable.

PROPOSITION 3.5. *Suppose that the stability parameters a_0, m_0 and s_0 satisfy*

$$a_0 \geq \underline{a}_0 > 0, \qquad m_0 \geq \underline{m}_0 > 0, \qquad s_0 > 0. \tag{3.3}$$

Then the discontinuous Galerkin method in (2.21)–(2.24) has a unique solution.

Proof: Since the discrete problem is linear and finite-dimensional, it is enough to show that the discontinuous Galerkin approximation to the incompressible MHD problem (2.1)–(2.4) with zero data, i.e., with $\mathbf{f} = \mathbf{g} = \mathbf{u}_D = \mathbf{b}_D = \mathbf{0}$ and $p_N = 0$, is given by $(\mathbf{u}_h, \mathbf{b}_h, p_h, r_h) = (\mathbf{0}, \mathbf{0}, 0, 0)$.

To show this, we choose the test function $(\mathbf{v}, \mathbf{c}, q, s) = (\mathbf{u}_h, \mathbf{b}_h, p_h, r_h)$ in the weak formulation (2.21)–(2.24). Adding the first two of the resulting equations and subtracting the last two, we easily obtain that

$$A_h(\mathbf{u}_h, \mathbf{u}_h) + O_h(\mathbf{u}_h, \mathbf{u}_h) + M_h(\mathbf{b}_h, \mathbf{b}_h) + J_h(r_h, r_h) = 0. \tag{3.4}$$

From this identity and the coercivity results in Proposition 3.1, as well as the fact that $J_h(r_h, r_h) = s_0|r_h|_S^2$, we conclude that $\|\mathbf{u}_h\|_V = 0$, $|\mathbf{b}_h|_C = 0$ and $|r_h|_S = 0$. This implies that $\mathbf{u}_h = \mathbf{0}$, $\mathbf{b}_h \in \mathbf{C}_h^c$ and $r_h \in S_h^c$. Hence, the fourth equation (2.24) now reads $D_h(\mathbf{b}_h, s) = 0$ for all $s \in S_h$. This also holds true for any $s \in S_h^c$: $D_h(\mathbf{b}_h, s) = D(\mathbf{b}_h, s) = 0$ for all $s \in S_h^c$. We conclude that $\mathbf{b}_h$ belongs to the conforming kernel of D, i.e., $\mathbf{b}_h \in \mathbf{X}_h^c$. Therefore, the coercivity result in Proposition 3.4 and (3.4) yield $\mathbf{b}_h = \mathbf{0}$.

Using that $\mathbf{u}_h = \mathbf{b}_h = \mathbf{0}$, the first equation (2.21) is reduced to $B_h(\mathbf{v}, p_h) = 0$ for all $\mathbf{v} \in \mathbf{V}_h$. The discrete inf-sup condition for B_h in Proposition 3.2 readily yields that $p_h = 0$. Finally, the second equation (2.22) is now $D_h(\mathbf{c}, r_h) = 0$ for all $\mathbf{c} \in \mathbf{C}_h$. Since $r_h \in S_h^c$, we also have $D_h(\mathbf{c}, r_h) = D(\mathbf{c}, r_h) = 0$ for any $\mathbf{c} \in \mathbf{C}_h^c$, and the inf-sup condition for D in Proposition 3.4 yields that $r_h = 0$. □

3.2. A-priori error estimates. Next, we state a-priori error estimates for the DG method in (2.21)–(2.24). To that end, we introduce the broken Sobolev space

$$H^\sigma(\mathcal{T}_h) = \{\, u \in L^2(\Omega) \,:\, u|_K \in H^\sigma(K),\ K \in \mathcal{T}_h \,\}, \qquad \sigma \geq 0,$$

and endow it with the broken norm

$$\|u\|^2_{\sigma,\mathcal{T}_h} = \sum_{K\in\mathcal{T}_h} \|u\|^2_{H^\sigma(K)}.$$

In our error analysis, we will suppose that the solution $(\mathbf{u}, \mathbf{b}, p, r) \in \mathbf{V} \times \mathbf{C} \times Q \times S$ of the MHD problem (2.1)–(2.4) satisfies

$$(\mathbf{u}, p) \in H^{\sigma+1}(\mathcal{T}_h)^3 \times H^\sigma(\mathcal{T}_h), \qquad \text{for } \sigma > \tfrac{1}{2}, \tag{3.5}$$

and

$$(\mathbf{b}, \nabla\times\mathbf{b}, r) \in H^\tau(\mathcal{T}_h)^3 \times H^\tau(\mathcal{T}_h)^3 \times H^{\tau+1}(\mathcal{T}_h), \qquad \text{for } \tau > \tfrac{1}{2}. \tag{3.6}$$

REMARK 3.6. *Let us point out that the regularity assumptions (3.5)–(3.6) are realistic. Indeed, for the Stokes problem in polyhedral domains (with square-integrable right-hand sides and $\Gamma_N = \emptyset$), the regularity property (3.5) has been proven in [16]. Furthermore, for Maxwell's equations in polyhedral domains, the embedding results in [1] show that the fields $\mathbf{b}$ and $\nabla\times\mathbf{b}$ can be expected to belong to $H^\tau(\mathcal{T}_h)^3$ for a regularity exponent $\tau > \frac{1}{2}$. In particular, this regularity assumption holds true for the strongest magnetic singularities in non-convex polyhedral domains. Finally, since r satisfies the Laplace problem (2.13), the assumption $r \in H^{\tau+1}(\mathcal{T}_h)$ is realistic as well, provided that the right-hand side $\mathbf{g}$ is in $H(\mathrm{div};\Omega)$.*

The following theorem represents the main theoretical result of this article.

THEOREM 3.7. *Let the solution $(\mathbf{u}, \mathbf{b}, p, r)$ of the MHD problem (2.1)–(2.4) satisfy the regularity assumptions in (3.5) and (3.6). Let $(\mathbf{u}_h, \mathbf{b}_h, p_h, r_h)$ denote the DG approximation defined in (2.21)–(2.24) with stability parameters satisfying (3.3). Then, the error in $\mathbf{u}$, $\mathbf{b}$ and r can be bounded by*

$$\begin{aligned}
&\|\mathbf{u}-\mathbf{u}_h\|_V + \|\mathbf{b}-\mathbf{b}_h\|_C + \|r-r_h\|_S \\
&\quad\leq Ch^{\min\{\sigma,k\}} \left(\left(\nu^{\frac{1}{2}} + \min\{1, \nu^{-\frac{1}{2}}h + h^{\frac{1}{2}}\}\right)\|\mathbf{u}\|_{\sigma+1,\mathcal{T}_h} + \nu^{-\frac{1}{2}}\|p\|_{\sigma,\mathcal{T}_h}\right) \\
&\quad + Ch^{\min\{\tau,k\}}\left(\|\mathbf{b}\|_{\tau,\mathcal{T}_h} + \|\nabla\times\mathbf{b}\|_{\tau,\mathcal{T}_h} + \|r\|_{\tau+1,\mathcal{T}_h}\right).
\end{aligned}$$

Moreover, the error in p satisfies

$$\begin{aligned}
\|p-p_h\|_{L^2(\Omega)} &\leq Ch^{\min\{\sigma,k\}}\left(\|\mathbf{u}\|_{\sigma+1,\mathcal{T}_h} + \nu^{-\frac{1}{2}}\|p\|_{\sigma,\mathcal{T}_h}\right) \\
&\quad + Ch^{\min\{\tau,k\}}\left(\|\mathbf{b}\|_{\tau,\mathcal{T}_h} + \|\nabla\times\mathbf{b}\|_{\tau,\mathcal{T}_h} + \|r\|_{\tau+1,\mathcal{T}_h}\right).
\end{aligned}$$

The constants $C > 0$ are independent of the mesh size and ν.

REMARK 3.8. *For smooth solutions, the estimate in Theorem 3.7 ensures convergence rates of order $\mathcal{O}(h^k)$ in the mesh size h. This rate is optimal in the approximation of the velocity, the pressure and the magnetic field in the respective norms, but suboptimal by one order in the approximation of the multiplier r with respect to the norm $\|\cdot\|_S$. This is due to the fact that we are using polynomials of degree $k+1$*

to approximate r. The same suboptimal result is observed for the conforming Nédélec family of the second type [33]. On the other hand, the use of polynomials of degree $k+1$ for the magnetic multiplier leads to optimal convergence rates in the L^2-error in the magnetic field $\mathbf{b}$, in contrast to the use polynomials of degree k, cf. the discussion in [27, 28].

REMARK 3.9. *The coefficient $\nu^{\frac{1}{2}}+\min\{1,\nu^{-\frac{1}{2}}h+h^{\frac{1}{2}}\}$ in front of $\|\mathbf{u}\|_{\sigma+1,\mathcal{T}_h}$ on the right-hand side in the first estimate in Theorem 3.7 corresponds to the approximation of the diffusion term and the convection term, respectively. With respect to convection, it is slightly suboptimal when compared to the standard error estimate for DG methods for pure convection equations, cf. [30]. The sub-optimality is due to the appearance of the pressure.*

4. Proofs. In this section, we shall prove the a-priori error estimate stated in Theorem 3.7. In Section 4.1, we introduce extended DG forms and discuss the resulting error equations. Continuity properties of the coupling and convection forms will be established in Section 4.2. Finally, in Section 4.3, we complete the proof of Theorem 3.7 in several steps.

4.1. Extended forms and error equations. For the purpose of our analysis, we set

$$\mathbf{V}(h)=\mathbf{V}+\mathbf{V}_h,\qquad \mathbf{C}(h)=\mathbf{C}+\mathbf{C}_h,\qquad S(h)=S+S_h.$$

Using the lifting operators constructed in [3, 36] and [27, 28], it is then possible to extend the discrete bilinear forms A_h, B_h, M_h, D_h to bilinear forms

$$\widetilde{A}_h:\mathbf{V}(h)\times\mathbf{V}(h)\to\mathbb{R},\qquad \widetilde{B}_h:\mathbf{V}(h)\times Q\to\mathbb{R},$$
$$\widetilde{M}_h:\mathbf{C}(h)\times\mathbf{C}(h)\to\mathbb{R},\qquad \widetilde{D}_h:\mathbf{C}(h)\times S(h)\to\mathbb{R},$$

respectively. The extended forms have the following continuity properties.

PROPOSITION 4.1. *The bilinear forms $\widetilde{A}_h$, $\widetilde{M}_h$, $\widetilde{B}_h$ and $\widetilde{D}_h$ satisfy*

$$\begin{aligned}
&|\widetilde{A}_h(\mathbf{u},\mathbf{v})|\le C\,\nu\|\mathbf{u}\|_{1,h}\,\|\mathbf{v}\|_{1,h} && \forall\,\mathbf{u},\mathbf{v}\in\mathbf{V}(h),\\
&|\widetilde{M}_h(\mathbf{b},\mathbf{c})|\le C\,|\mathbf{b}|_C\,|\mathbf{c}|_C && \forall\,\mathbf{b},\mathbf{c}\in\mathbf{C}(h),\\
&|\widetilde{B}_h(\mathbf{u},q)|\le C\|\mathbf{u}\|_{1,h}\,\|q\|_{L^2(\Omega)} && \forall\,\mathbf{u}\in\mathbf{V}(h),\ q\in Q,\\
&|\widetilde{D}_h(\mathbf{c},r)|\le C\,\|\mathbf{c}\|_C\,\|r\|_S && \forall\,\mathbf{c}\in\mathbf{C}(h),\ r\in S(h),
\end{aligned}$$

respectively, with constants $C>0$ that are independent of the mesh size, ν, ν_m and κ, and only depend on the stabilization parameters a_0, m_0, the shape-regularity constants of the meshes, and the polynomial degree k.

Moreover, the extended forms are constructed in such a way that

$$\begin{aligned}
&\widetilde{A}_h(\mathbf{u},\mathbf{v})=A_h(\mathbf{u},\mathbf{v}), && \widetilde{M}_h(\mathbf{b},\mathbf{c})=M_h(\mathbf{b},\mathbf{c}),\\
&\widetilde{B}_h(\mathbf{u},p)=B_h(\mathbf{u},p), && \widetilde{D}_h(\mathbf{b},r)=D_h(\mathbf{b},r),
\end{aligned}\tag{4.1}$$

for all discrete functions $\mathbf{u},\mathbf{v}\in\mathbf{V}_h$, $\mathbf{b},\mathbf{c}\in\mathbf{C}_h$, $p\in Q_h$ and $r\in S_h$, as well as

$$\begin{aligned}
&\widetilde{A}_h(\mathbf{u},\mathbf{v})=A(\mathbf{u},\mathbf{v}), && \widetilde{M}_h(\mathbf{b},\mathbf{c})=M(\mathbf{b},\mathbf{c}),\\
&\widetilde{B}_h(\mathbf{u},p)=B(\mathbf{u},p), && \widetilde{D}_h(\mathbf{b},r)=D(\mathbf{b},r),
\end{aligned}\tag{4.2}$$

for all $\mathbf{u}, \mathbf{v} \in \mathbf{V}$, $\mathbf{b}, \mathbf{c} \in \mathbf{C}$, $p \in Q$ and $r \in S$.

Suppose now that $(\mathbf{u}, \mathbf{b}, p, r)$ is the solution of the MHD problem (2.1)–(2.4). We define, for any $\mathbf{v} \in \mathbf{V}_h$, $\mathbf{c} \in \mathbf{C}_h$ and $s \in S_h$, the following functionals

$$\begin{aligned}
\mathcal{R}_A(\mathbf{v}) &= \widetilde{A}_h(\mathbf{u}, \mathbf{v}) + O_h(\mathbf{u}, \mathbf{v}) + C_h(\mathbf{v}, \mathbf{b}) + \widetilde{B}_h(\mathbf{v}, p) - F_h(\mathbf{v}), \\
\mathcal{R}_M(\mathbf{c}) &= \widetilde{M}_h(\mathbf{b}, \mathbf{c}) - C_h(\mathbf{u}, \mathbf{c}) + \widetilde{D}_h(\mathbf{c}, r) - G_h(\mathbf{c}), \\
\mathcal{R}_D(s) &= \widetilde{D}_h(\mathbf{b}, s) - J_h(r, s).
\end{aligned}$$

The terms $\mathcal{R}_A$, $\mathcal{R}_M$ and $\mathcal{R}_D$ measure how well the analytical solution satisfies the DG formulation when it is rewritten in terms of the extended bilinear forms. If now $(\mathbf{u}_h, \mathbf{b}_h, p_h, r_h)$ is the DG approximation, the following error equations are obtained from property (4.1): there holds

$$\mathcal{R}_A(\mathbf{v}) = \widetilde{A}_h(\mathbf{u} - \mathbf{u}_h, \mathbf{v}) + O_h(\mathbf{u} - \mathbf{u}_h, \mathbf{v}) + C_h(\mathbf{v}, \mathbf{b} - \mathbf{b}_h) + \widetilde{B}_h(\mathbf{v}, p - p_h), \quad (4.3)$$

$$\mathcal{R}_M(\mathbf{c}) = \widetilde{M}_h(\mathbf{b} - \mathbf{b}_h, \mathbf{c}) - C_h(\mathbf{u} - \mathbf{u}_h, \mathbf{c}) + \widetilde{D}_h(\mathbf{c}, r - r_h), \quad (4.4)$$

$$\mathcal{R}_D(s) = \widetilde{D}_h(\mathbf{b} - \mathbf{b}_h, s) - J_h(r - r_h, s), \quad (4.5)$$

for any $\mathbf{v} \in \mathbf{V}_h$, $\mathbf{c} \in \mathbf{C}_h$, and $S \in S_h$. We remark that the third equation (2.23) is consistent when it is rewritten in terms of the form $\widetilde{B}_h$. That is, from the definition of $\widetilde{B}_h$ in [36] we readily see that

$$\widetilde{B}_h(\mathbf{u}, q) = \langle \mathbf{u}_D \cdot \mathbf{n}, q \rangle_{\Gamma_D}, \qquad q \in Q_h.$$

Therefore, by (2.23) and (4.1), we have

$$\widetilde{B}_h(\mathbf{u} - \mathbf{u}_h, q) = 0, \qquad q \in Q_h. \quad (4.6)$$

Proceeding as in [27, 28, 36], we readily obtain the following bounds for $\mathcal{R}_A$, $\mathcal{R}_M$ and $\mathcal{R}_D$, respectively.

PROPOSITION 4.2. *Let the solution $(\mathbf{u}, \mathbf{b}, p, r)$ of the MHD problem satisfy the smoothness assumptions in (3.5) and (3.6). Then, we have*

$$\begin{aligned}
|\mathcal{R}_A(\mathbf{v})| &\le 2\nu^{\frac{1}{2}} |\mathbf{v}|_{V^\perp} \mathcal{E}(\mathbf{u}, \mathbf{b}, p), \\
|\mathcal{R}_M(\mathbf{c})| &\le |\mathbf{c}|_{C^\perp} \mathcal{E}(\mathbf{u}, \mathbf{b}, p), \\
|\mathcal{R}_D(s)| &\le |s|_S \mathcal{E}(\mathbf{u}, \mathbf{b}, p),
\end{aligned}$$

for all $\mathbf{v} \in \mathbf{V}_h$, $\mathbf{c} \in \mathbf{C}_h$ and $s \in S_h$, where $\mathcal{E}(\mathbf{u}, \mathbf{b}, p)$ can be bounded by

$$\begin{aligned}
\mathcal{E}(\mathbf{u}, \mathbf{b}, p) \le\ & C h^{\min\{\sigma, k\}} \left(\nu^{\frac{1}{2}} \|\mathbf{u}\|_{\sigma+1, \mathcal{T}_h} + \nu^{-\frac{1}{2}} \|p\|_{\sigma, \mathcal{T}_h} \right) \\
& + C h^{\min\{\tau, k\}} \left((\kappa \nu_m)^{\frac{1}{2}} (h \|\mathbf{b}\|_{\tau, \mathcal{T}_h} + \|\nabla \times \mathbf{b}\|_{\tau, \mathcal{T}_h}) \right),
\end{aligned}$$

with constants $C > 0$ that are independent of the mesh size, ν, ν_m and κ.

4.2. Continuity of coupling and convection forms. In this section, we establish some continuity properties of the coupling and convection forms. To that end, we introduce the additional norms:

$$\begin{aligned}
\|\mathbf{u}\|_\star^2 &= \|\mathbf{u}\|_{L^2(\Omega)}^2 + \sum_{K \in \mathcal{T}_h} h_K \|\mathbf{u}\|_{L^2(\partial K)}^2, \\
\|\mathbf{u}\|_O^2 &= \nu^{-1} \|\mathbf{u}\|_{L^2(\Omega)}^2 + \sum_{K \in \mathcal{T}_h} \|\mathbf{u}\|_{L^2(\partial K)}^2.
\end{aligned} \quad (4.7)$$

PROPOSITION 4.3. *There holds:*

$$|C_h(\mathbf{u},\mathbf{b})| \le C\|\mathbf{u}\|_\star |\mathbf{b}|_C \qquad \forall\, \mathbf{u}\in \mathbf{V}(h),\ \mathbf{b}\in \mathbf{C}(h),$$
$$|C_h(\mathbf{u},\mathbf{b})| \le C\|\mathbf{u}\|_{L^2(\Omega)} |\mathbf{b}|_C \qquad \forall\, \mathbf{u}\in \mathbf{V}_h,\ \mathbf{b}\in \mathbf{C}(h),$$

with a constant $C>0$ independent of the mesh size and ν.

Proof: Applying the Cauchy-Schwarz inequality and taking into account the shape-regularity of the meshes, we obtain

$$\begin{aligned}|C_h(\mathbf{u},\mathbf{b})| &\le \kappa\|\mathbf{d}\|_{L^\infty(\Omega)}\|\mathbf{u}\|_{L^2(\Omega)}\|\nabla\times\mathbf{b}\|_{L^2(\Omega)}\\ &\quad + C\kappa\|\mathbf{d}\|_{L^\infty(\Omega)}\left(\sum_{K\in\mathcal{T}_h}\int_{\partial K\setminus\Gamma_D} h_K|\mathbf{u}|^2\,ds\right)^{\frac12}\|h_F^{-\frac12}[\![\mathbf{b}]\!]_T\|_{L^2(F)}\\ &\le C\kappa^{\frac12}\nu_m^{-\frac12}\|\mathbf{d}\|_{L^\infty(\Omega)}\|\mathbf{u}\|_\star|\mathbf{b}|_C.\end{aligned}$$

To prove the second continuity estimate, we use the following discrete trace inequality: for any polynomial $u\in\mathcal{P}_k(K)$, $K\in\mathcal{T}_h$, we have

$$\|u\|_{L^2(\partial K)} \le Ch_K^{-\frac12}\|u\|_{L^2(K)}. \tag{4.8}$$

The constant $C>0$ only depends on the polynomial degree k and the shape-regularity constants of the meshes. We then readily obtain that

$$\|\mathbf{u}\|_\star \le C\|\mathbf{u}\|_{L^2(\Omega)} \qquad \forall\,\mathbf{u}\in\mathbf{V}_h. \tag{4.9}$$

With this bound, the second estimate of the proposition follows from the first one. □

Finally, we provide the following continuity properties for the convection form.

PROPOSITION 4.4. *Assume (2.5) and (2.12) hold. Then, the bilinear form O_h satisfies*

$$|O_h(\mathbf{u},\mathbf{v})| \le C\|\mathbf{u}\|_{1,h}\|\mathbf{v}\|_{L^2(\Omega)} \qquad \forall\,\mathbf{u}\in\mathbf{V}(h),\ \mathbf{v}\in\mathbf{V}_h,$$
$$|O_h(\mathbf{u},\mathbf{v})| \le C\|\mathbf{u}\|_O\|\mathbf{v}\|_V \qquad \forall\,\mathbf{u}\in\mathbf{V}(h),\ \mathbf{v}\in\mathbf{V}_h.$$

The constants $C>0$ are independent of the mesh size and ν.

Proof: Applying the Cauchy-Schwarz inequality to the form O_h in (2.26) yields

$$\begin{aligned}|O_h(\mathbf{u},\mathbf{v})| &\le \big(\|\mathbf{w}\|_{L^\infty(\Omega)}\|\mathbf{u}\|_{1,h} + \|\gamma\|_{L^\infty(\Omega)}\|\mathbf{u}\|_{L^2(\Omega)}\big)\,\|\mathbf{v}\|_{L^2(\Omega)}\\ &\quad + \|\mathbf{w}\|_{L^\infty(\Omega)}\sum_{K\in\mathcal{T}_h}\|h_K^{-\frac12}[\![\mathbf{u}]\!]\|_{L^2(\partial K_-\setminus\Gamma_-)}\,\|h_K^{\frac12}\mathbf{v}\|_{L^2(\partial K_-\setminus\Gamma_-)}\\ &\quad + \|\mathbf{w}\|_{L^\infty(\Omega)}\sum_{K\in\mathcal{T}_h}\|h_K^{-\frac12}\mathbf{u}\|_{L^2(\partial K_-\cap\Gamma_-)}\,\|h_K^{\frac12}\mathbf{v}\|_{L^2(\partial K_-\cap\Gamma_-)}.\end{aligned}$$

Using the Cauchy-Schwarz inequality, the shape-regularity of the mesh and the discrete trace inequality (4.8) for $\mathbf{v}\in\mathbf{V}_h$, we obtain

$$\sum_{K\in\mathcal{T}_h}\|h_K^{-\frac12}[\![\mathbf{u}]\!]\|_{L^2(\partial K_-\setminus\Gamma_-)}\,\|h_K^{\frac12}\mathbf{v}\|_{L^2(\partial K_-\setminus\Gamma_-)} \le C\Big(\sum_{F\in\mathcal{F}_h^I}h_F^{-1}\|[\![\mathbf{u}]\!]\|^2_{L^2(F)}\Big)^{\frac12}\|\mathbf{v}\|_{L^2(\Omega)}.$$

We proceed similarly for the boundary terms, but also take into account assumption (2.12) which implies that $\Gamma_- \subseteq \Gamma_D$. We obtain

$$\sum_{K\in\mathcal{T}_h} \|h_K^{-\frac{1}{2}}\mathbf{u}\|_{L^2(\partial K_-\cap\Gamma_-)}\, \|h_K^{\frac{1}{2}}\mathbf{v}\|_{L^2(\partial K_-\cap\Gamma_-)} \leq C\big(\sum_{F\in\mathcal{F}_h^D} h_F^{-1}\|[\![\mathbf{u}]\!]\|^2_{L^2(F)}\big)^{\frac{1}{2}}\|\mathbf{v}\|_{L^2(\Omega)}.$$

Therefore,

$$|O_h(\mathbf{u},\mathbf{v})| \leq C\left(\|\mathbf{w}\|_{L^\infty(\Omega)}\|\mathbf{u}\|_{1,h} + \|\gamma\|_{L^\infty(\Omega)}\|\mathbf{u}\|_{L^2(\Omega)}\right)\|\mathbf{v}\|_{L^2(\Omega)}.$$

The first continuity property of the proposition is achieved by applying the Poincaré inequality for piecewise smooth functions, cf. [5, Remark 1.1]:

$$\|\mathbf{u}\|_{L^2(\Omega)} \leq C\|\mathbf{u}\|_{1,h} \qquad \forall\, \mathbf{u}\in\mathbf{V}(h), \tag{4.10}$$

with $C>0$ only depending on the shape-regularity constants of the mesh.

To show the second estimate, we start from the integrated version (2.27) of the form O_h. Taking into account (2.5), we obtain

$$\begin{aligned}
|O_h(\mathbf{u},\mathbf{v})| &\leq \|\mathbf{w}\|_{L^\infty(\Omega)}\|\mathbf{u}\|_{L^2(\Omega)}\|\mathbf{v}\|_{1,h} + \|\gamma_0^{-\frac{1}{2}}(\gamma-\nabla\cdot\mathbf{w})\|_{L^\infty(\Omega)}\|\mathbf{u}\|_{L^2(\Omega)}\|\gamma_0^{\frac{1}{2}}\mathbf{v}\|_{L^2(\Omega)}\\
&\quad + \|\mathbf{w}\|^{\frac{1}{2}}_{L^\infty(\Omega)}\big(\sum_{K\in\mathcal{T}_h}\|\mathbf{u}\|^2_{L^2(\partial K_+\setminus\Gamma_+)}\big)^{\frac{1}{2}}\big(\sum_{K\in\mathcal{T}_h}\||\mathbf{w}\cdot\mathbf{n}_K|^{\frac{1}{2}}[\![\mathbf{v}]\!]\|^2_{L^2(\partial K_+\setminus\Gamma_+)}\big)^{\frac{1}{2}}\\
&\quad + \|\mathbf{w}\|^{\frac{1}{2}}_{L^\infty(\Omega)}\big(\sum_{K\in\mathcal{T}_h}\|\mathbf{u}\|^2_{L^2(\partial K_+\cap\Gamma_+)}\big)^{\frac{1}{2}}\||\mathbf{w}\cdot\mathbf{n}|^{\frac{1}{2}}\mathbf{v}\|_{L^2(\Gamma_+)}.
\end{aligned}$$

Using the Cauchy-Schwarz inequality for sums, we conclude that

$$\begin{aligned}
|O_h(\mathbf{u},\mathbf{v})| &\leq \|\mathbf{w}\|_{L^\infty(\Omega)}\|\mathbf{u}\|_{L^2(\Omega)}\|\mathbf{v}\|_{1,h} + \|\gamma_0^{-\frac{1}{2}}(\gamma-\nabla\cdot\mathbf{w})\|_{L^\infty(\Omega)}\|\mathbf{u}\|_{L^2(\Omega)}\|\gamma_0^{\frac{1}{2}}\mathbf{v}\|_{L^2(\Omega)}\\
&\quad + \|\mathbf{w}\|^{\frac{1}{2}}_{L^\infty(\Omega)}\big(\sum_{K\in\mathcal{T}_h}\|\mathbf{u}\|^2_{L^2(\partial K_+)}\big)^{\frac{1}{2}}\big(\sum_{F\in\mathcal{F}_h}\||\mathbf{w}\cdot\mathbf{n}|^{\frac{1}{2}}[\![\mathbf{v}]\!]\|^2_{L^2(F)}\big)^{\frac{1}{2}}\\
&\leq C\|\mathbf{u}\|_O\|\mathbf{v}\|_V,
\end{aligned}$$

where we have used that $\|\mathbf{u}\|_{L^2(\Omega)} \leq C\nu^{-\frac{1}{2}}\|\mathbf{u}\|_{L^2(\Omega)} \leq C\|\mathbf{u}\|_O$. This proves the second continuity estimate. □

4.3. Error bounds. We are now ready to derive our error bounds. Throughout this section, we denote by $(\mathbf{u},\mathbf{b},p,r)$ the solution of the MHD problem (2.1)–(2.4) and by $(\mathbf{u}_h,\mathbf{b}_h,p_h,r_h)$ its DG approximation (2.21)–(2.24). We also assume that the regularity assumptions in (3.5) and (3.6) hold. We split the velocity error as follows:

$$\mathbf{u}-\mathbf{u}_h = \mathbf{u}-\mathbf{\Pi}_B\mathbf{u}+\mathbf{\Pi}_B\mathbf{u}-\mathbf{u}_h = \eta_\mathbf{u}+\xi_\mathbf{u}, \tag{4.11}$$

where we use the Brezzi-Douglas-Marini (BDM) projection $\mathbf{\Pi}_B$ onto $\mathbf{V}_h\cap H(\mathrm{div};\Omega)$ of degree k for the approximation of the velocity, see [6, Proposition III.3.6]. For the other fields, specific approximations will be chosen at a later point.

REMARK 4.5. *The reason why we use the BDM projection to approximate the velocity is that it yields an exactly divergence-free approximation [6]. This allows us to decouple the velocity error from the pressure error, without having to invoke the discrete inf-sup condition. This, in turn, is crucial for bounding the convection and coupling terms.*

For notational convenience, we introduce

$$\begin{aligned}\mathcal{O}(\mathbf{u}) &= \sup_{\mathbf{v}\in\mathbf{V}_h} \frac{O_h(\eta_{\mathbf{u}},\mathbf{v})}{\|\mathbf{v}\|_V},\\ \mathcal{A}(\mathbf{u})^2 &= \|\eta_{\mathbf{u}}\|_V^2 + \|\eta_{\mathbf{u}}\|_\star^2 + \mathcal{O}(\mathbf{u})^2,\\ |\!|\!|(\mathbf{b},p,r)|\!|\!|^2 &= \|\mathbf{b}\|_C^2 + \|p\|_Q^2 + \|r\|_S^2.\end{aligned} \tag{4.12}$$

Finally, we decompose $\mathbf{b}_h$ and r_h into

$$\mathbf{b}_h = \mathbf{b}_h^c + \mathbf{b}_h^\perp, \qquad r_h = r_h^c + r_h^\perp, \tag{4.13}$$

with $\mathbf{b}_h^c \in \mathbf{C}_h^c$, $\mathbf{b}_h^\perp \in \mathbf{C}_h^\perp$, $r_h^c \in S_h^c$ and $r_h^\perp \in S_h^\perp$, in accordance to the decomposition in (3.1).

4.3.1. Error in u and b. In this section, we estimate the error in $\mathbf{u}$ and $\mathbf{b}$. To this end, we prove two technical lemmas. The first one establishes a bound for $\xi_{\mathbf{u}}$ and the non-conforming functions $\mathbf{b}_h^\perp$ and $r_h^\perp$.

LEMMA 4.6. *There are constants $C>0$ and $C_\varepsilon>0$ independent of the mesh size and ν such that*

$$\begin{aligned}&\|\xi_{\mathbf{u}}\|_V^2 + |\mathbf{b}_h^\perp|_{C^\perp}^2 + |r_h^\perp|_S^2\\ &\quad\le \varepsilon\|\mathbf{b}-\mathbf{b}_h\|_C^2 + C_\varepsilon\|\eta_r\|_S^2 + C\big(\mathcal{E}(\mathbf{u},\mathbf{b},p)^2 + \mathcal{A}(\mathbf{u})^2 + |\!|\!|(\mathbf{b}-\mathbf{c},p-q,r-s)|\!|\!|^2\big),\end{aligned}$$

for any $\varepsilon>0$, $\mathbf{c}\in\mathbf{C}_h^c$, $q\in Q_h$, and $s\in S_h^c$. The constant C_ε depends on ε.

Proof: Fix $\mathbf{c}\in\mathbf{C}_h^c$, $q\in Q_h$, $s\in S_h^c$ and $\varepsilon>0$. In addition to (4.11), we write

$$\begin{aligned}\mathbf{b}-\mathbf{b}_h &= \mathbf{b}-\mathbf{c}+\mathbf{c}-\mathbf{b}_h = \eta_{\mathbf{b}}+\xi_{\mathbf{b}},\\ p-p_h &= p-q+q-p_h \;= \eta_p+\xi_p,\\ r-r_h &= r-s+s-r_h \;= \eta_r+\xi_r.\end{aligned} \tag{4.14}$$

We now proceed in the following steps.

Step 1: We first observe that, since the functions $\mathbf{b}_h^c$ and $\mathbf{c}$ are conforming in $\mathbf{C}_h^c$, we have

$$|\mathbf{b}_h^\perp|_{C^\perp} = |\mathbf{c}-\mathbf{b}_h^c-\mathbf{b}_h^\perp|_{C^\perp} = |\mathbf{c}-\mathbf{b}_h|_{C^\perp} \le |\xi_{\mathbf{b}}|_C. \tag{4.15}$$

Similarly, from the conformity of r_h^c and s in S_h^c,

$$|r_h^\perp|_S = |s-r_h^c-r_h^\perp|_S = |s-r_h|_S = |\xi_r|_S. \tag{4.16}$$

Taking into account (4.15)–(4.16), we have

$$\|\xi_{\mathbf{u}}\|_V^2 + |\mathbf{b}_h^\perp|_{C^\perp}^2 + |r_h^\perp|_S^2 \le \|\xi_{\mathbf{u}}\|_V^2 + |\xi_{\mathbf{b}}|_C^2 + |\xi_r|_S^2. \tag{4.17}$$

To bound the right-hand side of (4.17), we observe (4.1), use the stability results for $\widetilde{A}_h+O_h$, $\widetilde{M}_h$ in Proposition 3.1, the fact that $J_h(\xi_r,\xi_r)=s_0|\xi_r|_S^2$, and add and subtract the coupling and multiplier terms. Thereby, we obtain

$$\begin{aligned}&C_1\,\big(\|\xi_{\mathbf{u}}\|_V^2 + |\xi_{\mathbf{b}}|_C^2 + |\xi_r|_S^2\big)\\ &\qquad\le \widetilde{A}_h(\xi_{\mathbf{u}},\xi_{\mathbf{u}}) + O_h(\xi_{\mathbf{u}},\xi_{\mathbf{u}}) + C_h(\xi_{\mathbf{u}},\xi_{\mathbf{b}}) + \widetilde{B}_h(\xi_{\mathbf{u}},\xi_p)\\ &\qquad\quad + \widetilde{M}_h(\xi_{\mathbf{b}},\xi_{\mathbf{b}}) - C_h(\xi_{\mathbf{u}},\xi_{\mathbf{b}}) + \widetilde{D}_h(\xi_{\mathbf{b}},\xi_r)\\ &\qquad\quad - \widetilde{B}_h(\xi_{\mathbf{u}},\xi_p) - \widetilde{D}_h(\xi_{\mathbf{b}},\xi_r) + J_h(\xi_r,\xi_r).\end{aligned} \tag{4.18}$$

From (4.18), and the error equations in (4.3)–(4.6), we now readily conclude that

$$C_1 \left(\|\xi_{\mathbf{u}}\|_V^2 + |\xi_{\mathbf{b}}|_C^2 + |\xi_r|_S^2 \right) \leq T_1 + T_2 + T_3 + T_4, \tag{4.19}$$

where

$$\begin{aligned}
T_1 &= \mathcal{R}_A(\xi_{\mathbf{u}}) - \widetilde{A}(\eta_{\mathbf{u}}, \xi_{\mathbf{u}}) - O_h(\eta_{\mathbf{u}}, \xi_{\mathbf{u}}) - C_h(\xi_{\mathbf{u}}, \eta_{\mathbf{b}}) - \widetilde{B}_h(\xi_{\mathbf{u}}, \eta_p), \\
T_2 &= \mathcal{R}_M(\xi_{\mathbf{b}}) - \widetilde{M}_h(\eta_{\mathbf{b}}, \xi_{\mathbf{b}}) + C_h(\eta_{\mathbf{u}}, \xi_{\mathbf{b}}) - \widetilde{D}_h(\xi_{\mathbf{b}}, \eta_r), \\
T_3 &= \widetilde{B}_h(\eta_{\mathbf{u}}, \xi_p), \\
T_4 &= -\mathcal{R}_D(\xi_r) + \widetilde{D}_h(\eta_{\mathbf{b}}, \xi_r) - J_h(\eta_r, \xi_r).
\end{aligned}$$

Step 2: We now bound the terms T_1, T_2, T_3 and T_4 under the additional assumption that $\mathbf{c}$ belongs to the kernel $\mathbf{X}_h^c$ defined in (3.2).

To bound T_1, we use the estimate of $\mathcal{R}_A$ in Proposition 4.2, the continuity properties of $\widetilde{A}_h$ and $\widetilde{B}_h$ in Proposition 4.1, the results for C_h in Proposition 4.3, and the estimates for O_h in Proposition 4.4. Upon application of the arithmetic-geometric mean inequality, we readily obtain that

$$\begin{aligned}
|T_1| &\leq C\|\xi_{\mathbf{u}}\|_V \big(\mathcal{E}(\mathbf{u}, \mathbf{b}, p) + \nu^{\frac{1}{2}} \|\eta_{\mathbf{u}}\|_{1,h} + \mathcal{O}(\mathbf{u}) + |\eta_{\mathbf{b}}|_C + \|\eta_p\|_Q \big) \\
&\leq \frac{C_1}{2} \|\xi_{\mathbf{u}}\|_V^2 + C\big(\mathcal{E}(\mathbf{u}, \mathbf{b}, p)^2 + \|\eta_{\mathbf{u}}\|_V^2 + \mathcal{O}(\mathbf{u})^2 + \|\eta_{\mathbf{b}}\|_C^2 + \|\eta_p\|_Q^2 \big).
\end{aligned} \tag{4.20}$$

Similarly, from Proposition 4.2, Proposition 4.1 and Proposition 4.3, we have

$$\begin{aligned}
|T_2| &\leq C|\xi_{\mathbf{b}}|_C \big(\mathcal{E}(\mathbf{u}, \mathbf{b}, p) + |\eta_{\mathbf{b}}|_C + \|\eta_{\mathbf{u}}\|_\star \big) + C\|\xi_{\mathbf{b}}\|_C \|\eta_r\|_S \\
&\leq C|\xi_{\mathbf{b}}|_C \big(\mathcal{E}(\mathbf{u}, \mathbf{b}, p) + \|\eta_{\mathbf{b}}\|_C + \|\eta_{\mathbf{u}}\|_\star \big) + C\|\mathbf{b} - \mathbf{b}_h\|_C \|\eta_r\|_S + C\|\eta_{\mathbf{b}}\|_C \|\eta_r\|_S.
\end{aligned}$$

Using the arithmetic-geometric mean inequality again, we have that, for all $\varepsilon > 0$,

$$\begin{aligned}
|T_2| \leq{}& \frac{C_1}{2} |\xi_{\mathbf{b}}|_C^2 + \frac{C_1}{2} \varepsilon \|\mathbf{b} - \mathbf{b}_h\|_C^2 \\
&+ C_\varepsilon \|\eta_r\|_S^2 + C\big(\mathcal{E}(\mathbf{u}, \mathbf{b}, p)^2 + \|\eta_{\mathbf{u}}\|_\star^2 + \|\eta_{\mathbf{b}}\|_C^2 + \|\eta_r\|_S^2 \big).
\end{aligned} \tag{4.21}$$

Next, we claim that

$$T_3 = 0. \tag{4.22}$$

To see this, we note that $\eta_{\mathbf{u}} = \mathbf{u} - \mathbf{\Pi}_B \mathbf{u}$ belongs to $H(\mathrm{div}; \Omega)$. It follows that $[\![\eta_{\mathbf{u}}]\!]_N = 0$ on interior faces. In addition, by virtue of [6, Proposition III.3.7] and since $\nabla \cdot \mathbf{u} = 0$, we have that

$$\nabla \cdot \eta_{\mathbf{u}} = \nabla \cdot (\mathbf{u} - \mathbf{\Pi}_B \mathbf{u}) = \Pi_{k-1}(\nabla \cdot \mathbf{u}) = 0 \qquad \text{in } \Omega.$$

Then, using the definition of $\widetilde{B}_h$ in [36] and the defining properties of the BDM projection (cf. [6, Proposition III.3.6]), we conclude that

$$T_3 = \widetilde{B}_h(\eta_{\mathbf{u}}, \xi_p) = \sum_{F \in \mathcal{F}_h^D} \int_F \eta_{\mathbf{u}} \cdot \mathbf{n}\, \xi_p \, ds = 0;$$

thereby, proving (4.22) holds.

For the term T_4, we first note, since $s \in S_h^c$, we have $J_h(\eta_r, \xi_r) = 0$. Furthermore,

$$\widetilde{D}_h(\eta_{\mathbf{b}}, \xi_r) = \widetilde{D}_h(\eta_{\mathbf{b}}, s - r_h) = \widetilde{D}_h(\eta_{\mathbf{b}}, s - r_h^c) - \widetilde{D}_h(\eta_{\mathbf{b}}, r_h^\perp).$$

From property (4.2), we conclude that

$$\widetilde{D}_h(\eta_{\mathbf{b}}, s - r_h^c) = D(\mathbf{b}, s - r_h^c) - D(\mathbf{c}, s - r_h^c).$$

Both terms on the right-hand side are zero: the first one due to the weak equation (2.17) and the second one due to the assumption that $\mathbf{c} \in \mathbf{X}_h^c$. As a consequence, we obtain

$$T_4 = -\mathcal{R}_D(\xi_r) - \widetilde{D}_h(\eta_{\mathbf{b}}, r_h^\perp).$$

From Proposition 4.2 and the continuity of $\widetilde{D}_h$ in Proposition 4.1,

$$|T_4| \leq C|\xi_r|_S \mathcal{E}(\mathbf{u}, \mathbf{b}, p) + C\|\eta_{\mathbf{b}}\|_C \|r_h^\perp\|_S.$$

The norm-equivalence in Proposition 3.3 and the identity (4.16) yield

$$\|r_h^\perp\|_S \leq C|r_h^\perp|_S = C|\xi_r|_S.$$

These results and the arithmetic-geometric mean inequality readily show that

$$|T_4| \leq \frac{C_1}{2}|\xi_r|_S^2 + C\left(\mathcal{E}(\mathbf{u}, \mathbf{b}, p)^2 + \|\eta_{\mathbf{b}}\|_C^2\right). \tag{4.23}$$

Combining the estimates in (4.19), (4.20), (4.21), (4.22) and (4.23) implies that

$$\begin{aligned}
&\frac{C_1}{2}\left(\|\xi_{\mathbf{u}}\|_V^2 + |\xi_{\mathbf{b}}|_C^2 + |\xi_r|_S^2\right) \\
&\qquad \leq \frac{C_1}{2}\varepsilon\|\mathbf{b} - \mathbf{b}_h\|_C^2 + C_\varepsilon\|\eta_r\|_S^2 \\
&\qquad\quad + C\Big(\mathcal{E}(\mathbf{u}, \mathbf{b}, p)^2 + \mathcal{A}(\mathbf{u})^2 + |\!|\!|(\mathbf{b} - \mathbf{c}, p - q, r - s)|\!|\!|^2\Big),
\end{aligned}$$

provided that $\mathbf{c} \in \mathbf{X}_h^c$. Dividing the previous estimate by $\frac{C_1}{2}$ and using (4.17) yield

$$\begin{aligned}
&\|\xi_{\mathbf{u}}\|_V^2 + |\mathbf{b}_h^\perp|_{C^\perp}^2 + |r_h^\perp|_S^2 \\
&\qquad \leq \varepsilon\|\mathbf{b} - \mathbf{b}_h\|_C^2 + C_\varepsilon\|\eta_r\|_S^2 \\
&\qquad\quad + C\big(\mathcal{E}(\mathbf{u}, \mathbf{b}, p)^2 + \mathcal{A}(\mathbf{u})^2 + |\!|\!|(\mathbf{b} - \mathbf{c}, p - q, r - s)|\!|\!|^2\big),
\end{aligned} \tag{4.24}$$

provided that $\mathbf{c} \in \mathbf{X}_h^c$.

Step 3: We show that, in estimate (4.24), the approximation $\mathbf{c} \in \mathbf{X}_h^c$ can be replaced by any $\mathbf{c} \in \mathbf{C}_h^c$. To that end, take $\mathbf{c} \in \mathbf{C}_h^c$ and look for $\mathbf{a} \in \mathbf{C}_h^c$ such that

$$\widetilde{D}_h(\mathbf{a}, s) = \widetilde{D}_h(\mathbf{b} - \mathbf{c}, s) \qquad \forall\, s \in S_h^c.$$

By Proposition 4.1, the right-hand side is a continuous functional on S_h^c. Since $\mathbf{X}_h^c$ is non-empty and $\widetilde{D}_h = D$ on $\mathbf{C}_h^c \times S_h^c$, cf. (4.2), the inf-sup condition for D in

Proposition 3.4 implies that there exists at least one non-trivial solution $\mathbf{a} \in \mathbf{C}_h^c$ satisfying

$$\|\mathbf{a}\|_C \leq C \, \|\mathbf{b} - \mathbf{c}\|_C,$$

with a constant $C > 0$ only depending on the continuity constant of $\widetilde{D}_h$ and the discrete inf-sup constant of D on $\mathbf{C}_h^c \times S_h^c$, see [6, Equation II.2.20]. By construction, we have $\mathbf{a} + \mathbf{c} \in \mathbf{X}_h^c$, since, due to (4.2) and (2.17), there holds

$$\widetilde{D}_h(\mathbf{b}, s) = D(\mathbf{b}, s) = 0 \qquad \forall \, s \in S_h^c.$$

Consequently, $(\mathbf{a} + \mathbf{c})$ can be used as an approximation in (4.24). By construction,

$$\|\mathbf{b} - (\mathbf{a} + \mathbf{c})\|_C \leq \|\mathbf{b} - \mathbf{c}\|_C + \|\mathbf{a}\|_C \leq C \, \|\mathbf{b} - \mathbf{c}\|_C,$$

and inequality (4.24) holds for any $\mathbf{c} \in \mathbf{C}_h^c$, which completes the proof. □

The second technical lemma of this subsection bounds the error in $\mathbf{b}$.

LEMMA 4.7. *There exists a constant $C > 0$ independent of the mesh size and ν such that*

$$\|\mathbf{b} - \mathbf{b}_h\|_C^2 \leq C\big(\|\xi_{\mathbf{u}}\|_V^2 + \|\eta_{\mathbf{u}}\|_\star^2 + |\mathbf{b}_h^\perp|_{C^\perp}^2 + |r_h^\perp|_S^2 + |\!|\!|(\mathbf{b} - \mathbf{c}, 0, r - s)|\!|\!|^2\big),$$

for any $\mathbf{c} \in \mathbf{C}_h^c$ and $s \in S_h^c$.

Proof: Let $\mathbf{c} \in \mathbf{C}^c$ and $s \in S_h^c$. Again, we split the errors in $\mathbf{b}$ and r into two parts and adopt the same notation as in (4.14). We now proceed in two steps.

Step 1: We first consider the case where the approximation $\mathbf{c} \in \mathbf{C}_h^c$ to the magnetic field $\mathbf{b}$ is such that

$$\mathbf{c} - \mathbf{b}_h^c \in \mathbf{X}_h^c. \tag{4.25}$$

It can be readily shown that non-trivial approximations of this type exist. To show this, consider the problem: find $\mathbf{c} \in \mathbf{C}_h^c$ such that

$$\widetilde{D}_h(\mathbf{c}, s) = \widetilde{D}_h(\mathbf{b}_h^c, s) \qquad \forall \, s \in S_h^c. \tag{4.26}$$

As before, the right-hand side is a continuous functional on S_h^c (see Proposition 4.1), and the discrete inf-sup condition for D (see (4.2) and Proposition 3.4) ensures that problem (4.26) admits at least one non-trivial solution $\mathbf{c} \in \mathbf{C}_h^c$ which then satisfies property (4.25).

Now let $\mathbf{c} \in \mathbf{C}_h^c$ be such that (4.25) holds. We decompose the function $\xi_{\mathbf{b}} = \mathbf{c} - \mathbf{b}_h$ into

$$\xi_{\mathbf{b}} = \xi_{\mathbf{b}}^c + \xi_{\mathbf{b}}^\perp, \qquad \xi_{\mathbf{b}}^c \in \mathbf{C}_h^c, \ \xi_{\mathbf{b}}^\perp \in \mathbf{C}_h^\perp, \tag{4.27}$$

according to (3.1). Since the approximation $\mathbf{c}$ belongs to the conforming space $\mathbf{C}_h^c$, we have

$$\xi_{\mathbf{b}}^c = (\mathbf{c} - \mathbf{b}_h^c), \qquad \xi_{\mathbf{b}}^\perp = -\mathbf{b}_h^\perp. \tag{4.28}$$

Next, we bound $\|\xi_{\mathbf{b}}^c\|_C$. Due to the coercivity of $\widetilde{M}_h$ on $\mathbf{C}_h$, see Proposition 3.1 and (4.1), and the fact that $\xi_{\mathbf{b}} = \xi_{\mathbf{b}}^c - \mathbf{b}_h^\perp$, we have

$$C_1 \|\xi_{\mathbf{b}}^c\|_C^2 \leq \widetilde{M}_h(\xi_{\mathbf{b}}^c, \xi_{\mathbf{b}}^c) = \widetilde{M}_h(\eta_{\mathbf{b}} + \xi_{\mathbf{b}}, \xi_{\mathbf{b}}^c) - \widetilde{M}_h(\eta_{\mathbf{b}}, \xi_{\mathbf{b}}^c) + \widetilde{M}_h(\mathbf{b}_h^\perp, \xi_{\mathbf{b}}^c).$$

Using the error equation in (4.4), we obtain that

$$\widetilde{M}_h(\eta_{\mathbf{b}}+\xi_{\mathbf{b}},\xi^c_{\mathbf{b}})=\mathcal{R}_M(\xi^c_{\mathbf{b}})+C_h(\eta_{\mathbf{u}}+\xi_{\mathbf{u}},\xi^c_{\mathbf{b}})-\widetilde{D}_h(\xi^c_{\mathbf{b}},\eta_r+\xi_r).$$

The term $\mathcal{R}_M(\xi^c_{\mathbf{b}})$ is zero because $\xi^c_{\mathbf{b}}\in\mathbf{C}^c_h$. Moreover, the term $-\widetilde{D}_h(\xi^c_{\mathbf{b}},\eta_r+\xi_r)$ can be simplified as follows: since $\xi^c_{\mathbf{b}}=\mathbf{c}-\mathbf{b}^c_h$ and $s\in S^c_h$, we deduce from (4.25) and (4.1) that

$$\begin{aligned}-\widetilde{D}_h(\xi^c_{\mathbf{b}},\eta_r+\xi_r)&=-\widetilde{D}_h(\xi^c_{\mathbf{b}},\eta_r)-\widetilde{D}_h(\xi^c_{\mathbf{b}},s-r^c_h-r^\perp_h)\\&=-\widetilde{D}_h(\xi^c_{\mathbf{b}},\eta_r)+\widetilde{D}_h(\xi^c_{\mathbf{b}},r^\perp_h).\end{aligned}$$

From the previous discussion, we conclude that

$$C_1\|\xi^c_{\mathbf{b}}\|^2_C\le S_1+S_2, \tag{4.29}$$

where

$$\begin{aligned}S_1&=-\widetilde{M}_h(\eta_{\mathbf{b}},\xi^c_{\mathbf{b}})+C_h(\eta_{\mathbf{u}},\xi^c_{\mathbf{b}})-\widetilde{D}_h(\xi^c_{\mathbf{b}},\eta_r),\\S_2&=\widetilde{M}_h(\mathbf{b}^\perp_h,\xi^c_{\mathbf{b}})+C_h(\xi_{\mathbf{u}},\xi^c_{\mathbf{b}})+\widetilde{D}_h(\xi^c_{\mathbf{b}},r^\perp_h).\end{aligned}$$

The continuity properties of $\widetilde{M}_h$, $\widetilde{D}_h$ and C_h in Proposition 4.1 and Proposition 4.3, respectively, and the arithmetic-geometric mean inequality yield

$$|S_1|\le\frac{C_1}{4}\|\xi^c_{\mathbf{b}}\|^2_C+C\big(|\eta_{\mathbf{b}}|^2_C+\|\eta_{\mathbf{u}}\|^2_\star+\|\eta_r\|^2_S\big). \tag{4.30}$$

Similarly,

$$\begin{aligned}|S_2|&\le\frac{C_1}{4}\|\xi^c_{\mathbf{b}}\|^2_C+C\big(\|\mathbf{b}^\perp_h\|^2_C+\|\xi_{\mathbf{u}}\|^2_{L^2(\Omega)}+\|r^\perp_h\|^2_S\big)\\&\le\frac{C_1}{4}\|\xi^c_{\mathbf{b}}\|^2_C+C\big(|\mathbf{b}^\perp_h|^2_{C^\perp}+\|\xi_{\mathbf{u}}\|^2_V+|r^\perp_h|^2_S\big),\end{aligned} \tag{4.31}$$

where we have also used the norm-equivalence results in Proposition 3.3.

Combining (4.29) with the estimates (4.30)–(4.31) shows that

$$\|\xi^c_{\mathbf{b}}\|^2_C\le C\big(\|\xi_{\mathbf{u}}\|^2_V+\|\eta_{\mathbf{u}}\|^2_\star+|\mathbf{b}^\perp_h|^2_{C^\perp}+|r^\perp_h|^2_S+|\!|\!|(\mathbf{b}-\mathbf{c},0,r-s)|\!|\!|^2\big).$$

Therefore, the previous estimate, the decomposition (4.27)–(4.28), the triangle inequality and the norm equivalence in Proposition 3.3 yield that

$$\begin{aligned}\|\mathbf{b}-\mathbf{b}_h\|^2_C&\le C(\|\eta_{\mathbf{b}}\|^2_C+\|\xi_{\mathbf{b}}\|^2_C)\\&\le C(\|\eta_{\mathbf{b}}\|^2_C+\|\xi^c_{\mathbf{b}}\|^2_C+|\mathbf{b}^\perp_h|^2_{C^\perp})\\&\le C(\|\xi_{\mathbf{u}}\|^2_V+\|\eta_{\mathbf{u}}\|^2_\star+|\mathbf{b}^\perp_h|^2_{C^\perp}+|r^\perp_h|^2_S+|\!|\!|(\mathbf{b}-\mathbf{c},0,r-s)|\!|\!|^2\big),\end{aligned} \tag{4.32}$$

for any $s\in S^c_h$ and $\mathbf{c}\in\mathbf{C}^c_h$ satisfying (4.25).

Step 2: We now show that (4.32) holds for $\mathbf{c}\in\mathbf{C}^c_h$ arbitrary. Proceeding as before, we can find a non-trivial function $\mathbf{a}\in\mathbf{C}^c_h$ such that

$$\begin{cases}\widetilde{D}_h(\mathbf{a},s)=\widetilde{D}_h(\mathbf{b}-\mathbf{c}-\mathbf{b}^\perp_h,s) & \forall\, s\in S^c_h,\\ \|\mathbf{a}\|_C\le C\,\big(\|\mathbf{b}-\mathbf{c}\|_C+\|\mathbf{b}^\perp_h\|_C\big).\end{cases} \tag{4.33}$$

Then, due to the properties in (4.1), (4.2) and the weak formulation in (2.17), (2.24), we have

$$D((\mathbf{a}+\mathbf{c})-\mathbf{b}_h^c,s)=\widetilde{D}_h((\mathbf{a}+\mathbf{c})-\mathbf{b}_h^c,s)=\widetilde{D}_h(\mathbf{b}-\mathbf{b_h},s)=D(\mathbf{b},s)-D_h(\mathbf{b}_h,s)=0,$$

for any $s\in S_h^c$. Hence, $(\mathbf{a}+\mathbf{c})-\mathbf{b}_h^c\in\mathbf{X}_h^c$ and $\mathbf{a}+\mathbf{c}$ satisfies (4.25). It can then be used as an approximation in (4.32). In view of (4.33) and the norm-equivalence in Proposition 3.3, we obtain

$$\|\mathbf{b}-(\mathbf{a}+\mathbf{c})\|_C\le\|\mathbf{b}-\mathbf{c}\|_C+\|\mathbf{a}\|_C\le C\|\mathbf{b}-\mathbf{c}\|_C+|\mathbf{b}_h^\perp|_{C^\perp}.$$

It follows that (4.32) holds for any approximation $\mathbf{c}\in\mathbf{C}_h^c$, which completes the proof of the lemma. □

We are now ready to bound the errors in $\mathbf{u}$ and $\mathbf{b}$.

THEOREM 4.8. *There exists a constant $C>0$, independent of the mesh size and ν such that*

$$\begin{aligned}\|\mathbf{u}-\mathbf{u}_h\|_V+\|\mathbf{b}-\mathbf{b}_h\|_C+|\mathbf{b}_h^\perp|_{C^\perp}+|r_h^\perp|_S\\ \le C\big(\,\mathcal{E}(\mathbf{u},\mathbf{b},p)+\mathcal{A}(\mathbf{u})+|\!|\!|(\mathbf{b}-\mathbf{c},p-q,r-s)|\!|\!|\,\big),\end{aligned}$$

for any $\mathbf{c}\in\mathbf{C}_h^c$, $q\in Q_h$ and $s\in S_h^c$.

Proof: Fix $\mathbf{c}\in\mathbf{C}_h^c$, $q\in Q_h$ and $s\in S_h^c$. Decomposing the errors as in (4.11) and (4.14), we obtain from the triangle inequality, Lemma 4.7 and Lemma 4.6:

$$\begin{aligned}&\|\mathbf{u}-\mathbf{u}_h\|_V^2+\|\mathbf{b}-\mathbf{b}_h\|_C^2+|\mathbf{b}_h^\perp|_{C^\perp}^2+|r_h^\perp|_S^2\\ &\quad\le C\left(\|\eta_{\mathbf{u}}\|_V^2+\|\xi_{\mathbf{u}}\|_V^2+\|\mathbf{b}-\mathbf{b}_h\|_C^2+|\mathbf{b}_h^\perp|_{C^\perp}^2+|r_h^\perp|_S^2\right)\\ &\quad\le C\left(\|\eta_{\mathbf{u}}\|_\star^2+\|\xi_{\mathbf{u}}\|_V^2+|\!|\!|(\mathbf{b}-\mathbf{c},0,r-s)|\!|\!|^2+|\mathbf{b}_h^\perp|_{C^\perp}^2+|r_h^\perp|_S^2\right)\\ &\quad\le C\varepsilon\|\mathbf{b}-\mathbf{b}_h\|_C^2+C_\varepsilon\|\eta_r\|_S^2\\ &\qquad+C\left(\mathcal{E}(\mathbf{u},p,\mathbf{b})^2+\mathcal{A}(\mathbf{u})^2+|\!|\!|(\mathbf{b}-\mathbf{c},p-q,r-s)|\!|\!|^2\right).\end{aligned}$$

Choosing $\varepsilon=\frac{1}{2C}$ and bringing the term $\frac{1}{2}\|\mathbf{b}-\mathbf{b}_h\|_C^2$ to the left-hand side now readily implies the assertion. □

4.3.2. Error in p and r. Next, we bound the errors in the pressure p and the multiplier r.

PROPOSITION 4.9. *There is a constant $C>0$ independent of the mesh size and ν such that*

$$\|p-p_h\|_{L^2(\Omega)}\le C\left(\mathcal{E}(\mathbf{u},\mathbf{b},p)+\mathcal{A}(\mathbf{u})+\|\eta_{\mathbf{u}}\|_{1,h}+|\!|\!|(\mathbf{b}-\mathbf{c},p-q,r-s)|\!|\!|\right),$$

for any $\mathbf{c}\in\mathbf{C}_h^c$, $q\in Q_h$ and $s\in S_h^c$.

Proof: Let $\mathbf{c}\in\mathbf{C}_h^c$, $q\in Q_h$ and $s\in S_h^c$. As before, we split the errors into two parts and adopt the same notation as in (4.14). Obviously, by the triangle inequality

$$\|p-p_h\|_{L^2(\Omega)}\le\|\eta_p\|_{L^2(\Omega)}+\|\xi_p\|_{L^2(\Omega)}.\tag{4.34}$$

We must then further estimate $\|\xi_p\|_{L^2(\Omega)}$. For reasons that will become clear below, we make use of the continuous inf-sup condition over $\mathbf{V}\times Q$, instead of the discrete one in Proposition 3.2. For $\Gamma_N=\emptyset$, a proof of the continuous inf-sup condition can

be found in [21]. The case $\Gamma_N \neq \emptyset$ follows similarly by subtracting pressure mean values. Therefore, we conclude that there is $\mathbf{v} \in \mathbf{V}$ such that

$$C\|\xi_p\|_{L^2(\Omega)} \leq \widetilde{B}_h(\mathbf{v}, \xi_p) \qquad \text{and} \qquad \|\mathbf{v}\|_{H^1(\Omega)} \leq 1, \tag{4.35}$$

where we have also used (4.2). We now set $\mathbf{v}_h = \mathbf{\Pi}_B \mathbf{v}$ with $\mathbf{\Pi}_B$ denoting the BDM projection into $\mathbf{V}_h \cap H(\mathrm{div}; \Omega)$. By using the definition of the extended form $\widetilde{B}_h$ in [36], (4.1), (4.2) and the properties of the BDM projection, we readily obtain

$$\widetilde{B}_h(\mathbf{v}_h, \xi_p) = \widetilde{B}_h(\mathbf{v}, \xi_p). \tag{4.36}$$

In addition, the approximation property of the BDM projection and (4.35) guarantee that

$$\|\mathbf{v}_h\|_{1,h} \leq \|\mathbf{v} - \mathbf{v}_h\|_{1,h} + \|\mathbf{v}\|_{1,h} \leq C\|\mathbf{v}\|_{H^1(\Omega)} \leq C. \tag{4.37}$$

In fact, the equations (4.36) and (4.37) imply the discrete inf-sup condition in Proposition 3.2 from the continuous one.

Now, we use the error equation (4.3) to obtain

$$\widetilde{B}_h(\mathbf{v}_h, \xi_p) = T_1 + T_2 + T_3, \tag{4.38}$$

where

$$\begin{aligned}
T_1 &= \mathcal{R}_A(\mathbf{v}_h) - \widetilde{A}_h(\eta_{\mathbf{u}}, \mathbf{v}_h) - O_h(\eta_{\mathbf{u}}, \mathbf{v}_h) - \widetilde{B}_h(\mathbf{v}_h, \eta_p), \\
T_2 &= -C_h(\mathbf{v}_h, \mathbf{b} - \mathbf{b}_h), \\
T_3 &= -\widetilde{A}_h(\xi_{\mathbf{u}}, \mathbf{v}_h), \\
T_4 &= -O_h(\xi_{\mathbf{u}}, \mathbf{v}_h).
\end{aligned}$$

We now bound T_1, T_2, T_3 and T_4.

For T_1, we use Proposition 4.2, the continuity results for $\widetilde{A}_h$ and $\widetilde{B}_h$ in Proposition 4.1 and the first continuity estimate for O_h in Proposition 4.4 combined with the Poincaré inequality (4.10). We obtain

$$\begin{aligned}
|T_1| &\leq C\|\mathbf{v}_h\|_{1,h} \left(\nu^{\frac{1}{2}} \mathcal{E}(\mathbf{u}, \mathbf{b}, p) + \nu\|\eta_{\mathbf{u}}\|_{1,h} + \|\eta_{\mathbf{u}}\|_{1,h} + \|\eta_p\|_{L^2(\Omega)} \right) \\
&\leq C \left(\nu^{\frac{1}{2}} \mathcal{E}(\mathbf{u}, \mathbf{b}, p) + \nu\|\eta_{\mathbf{u}}\|_{1,h} + \|\eta_{\mathbf{u}}\|_{1,h} + \|\eta_p\|_{L^2(\Omega)} \right),
\end{aligned} \tag{4.39}$$

where we have also used (4.37).

To estimate T_2, we use the continuity property of C_h in Proposition 4.3 and the Poincaré inequality (4.10):

$$|T_2| \leq C\|\mathbf{v}_h\|_{L^2(\Omega)} |\mathbf{b} - \mathbf{b}_h|_C \leq C\|\mathbf{v}_h\|_{1,h} \|\mathbf{b} - \mathbf{b}_h\|_C.$$

From Theorem 4.8 and (4.37), we thus conclude

$$|T_2| \leq C\big(\mathcal{E}(\mathbf{u}, \mathbf{b}, p) + \mathcal{A}(\mathbf{u}) + |\!|\!|(\mathbf{b} - \mathbf{c}, p - q, r - s)|\!|\!| \big). \tag{4.40}$$

To bound T_3, we use the continuity of $\widetilde{A}_h$ and Lemma 4.6 (with $\varepsilon = 1$). We conclude that

$$\begin{aligned}
|T_3| &\leq C\nu\|\mathbf{v}_h\|_{1,h} \|\xi_{\mathbf{u}}\|_{1,h} \\
&\leq C\nu^{\frac{1}{2}} \|\mathbf{v}_h\|_{1,h} \|\xi_{\mathbf{u}}\|_V \\
&\leq C\nu^{\frac{1}{2}} \|\mathbf{v}_h\|_{1,h} \left(\|\mathbf{b} - \mathbf{b}_h\|_C + \mathcal{E}(\mathbf{u}, \mathbf{b}, p) + \mathcal{A}(\mathbf{u}) + |\!|\!|(\mathbf{b} - \mathbf{c}, p - q, r - s)|\!|\!| \right).
\end{aligned}$$

The bound for $\|\mathbf{b}-\mathbf{b}_h\|_C$ in Theorem 4.8 and (4.37) thus give

$$|T_3| \le C\nu^{\frac{1}{2}} \left(\mathcal{E}(\mathbf{u},\mathbf{b},p) + \mathcal{A}(\mathbf{u}) + |\!|\!|(\mathbf{b}-\mathbf{c}, p-q, r-s)|\!|\!|\right). \tag{4.41}$$

The term T_4 is the reason for introducing the continuous field $\mathbf{v}$ in (4.34). To bound it, we proceed as follows. We use the integrated form (2.27) of O_h and write

$$O_h(\xi_{\mathbf{u}}, \mathbf{v}_h) = T_{4,1} + T_{4,2} + T_{4,3},$$

with

$$\begin{aligned}
T_{4,1} &= -\sum_{K\in\mathcal{T}_h} \int_K (\mathbf{w}\cdot\nabla)\mathbf{v}_h \cdot \xi_{\mathbf{u}}\, d\mathbf{x} + \sum_{K\in\mathcal{T}_h} \int_K (\gamma - \nabla\cdot\mathbf{w})\xi_{\mathbf{u}}\cdot\mathbf{v}_h\, d\mathbf{x},\\
T_{4,2} &= \sum_{K\in\mathcal{T}_h} \int_{\partial K_+\setminus\Gamma_+} \mathbf{w}\cdot\mathbf{n}_K \xi_{\mathbf{u}}\cdot(\mathbf{v}_h - \mathbf{v}_h^e)\, ds,\\
T_{4,3} &= \int_{\Gamma_+} \mathbf{w}\cdot\mathbf{n}\xi_{\mathbf{u}}\cdot\mathbf{v}_h\, ds.
\end{aligned}$$

With the Poincaré inequality (4.10), the term $T_{4,1}$ can be readily bounded by

$$|T_{4,1}| \le C\|\xi_{\mathbf{u}}\|_{L^2(\Omega)} \left(\|\mathbf{v}_h\|_{1,h} + \|\mathbf{v}_h\|_{L^2(\Omega)}\right) \le C\|\xi_{\mathbf{u}}\|_V \|\mathbf{v}_h\|_{1,h}.$$

For the term $T_{4,2}$, we use arguments as in the proof of Proposition 4.4 and the discrete trace inequality (4.8) to obtain

$$\begin{aligned}
|T_{4,2}| &\le C\|\mathbf{w}\|_{L^\infty(\Omega)} \Big(\sum_{K\in\mathcal{T}_h} h_K \|\xi_{\mathbf{u}}\|^2_{L^2(\partial K)}\Big)^{\frac{1}{2}} \Big(\sum_{F\in\mathcal{F}_h^I} h_F^{-1} \|[\![\mathbf{v}_h]\!]\|^2_{L^2(F)}\Big)^{\frac{1}{2}}\\
&\le C\|\mathbf{w}\|_{L^\infty(\Omega)} \|\xi_{\mathbf{u}}\|_{L^2(\Omega)} \|\mathbf{v}_h\|_{1,h} \le C\|\xi_{\mathbf{u}}\|_V \|\mathbf{v}_h\|_{1,h}.
\end{aligned}$$

Finally, the term $T_{4,3}$ can be written as

$$T_{4,3} = \int_{\Gamma_+} \mathbf{w}\cdot\mathbf{n}\xi_{\mathbf{u}}\cdot(\mathbf{v}_h - \mathbf{v})\, ds + \int_{\Gamma_+} \mathbf{w}\cdot\mathbf{n}\xi_{\mathbf{u}}\cdot\mathbf{v}\, ds,$$

with the continuous velocity field $\mathbf{v}$ from (4.35). For the first integral above, we use the approximation properties of the BDM projection in [6, Proposition III.3.6] and obtain

$$\begin{aligned}
\Big|\int_{\Gamma_+} \mathbf{w}\cdot\mathbf{n}\xi_{\mathbf{u}}\cdot(\mathbf{v}_h - \mathbf{v})\, ds\Big| &\le \Big(\int_\Gamma |\mathbf{w}\cdot\mathbf{n}||\xi_{\mathbf{u}}|^2\, ds\Big)^{\frac{1}{2}} \Big(\int_\Gamma |\mathbf{w}\cdot\mathbf{n}||\mathbf{v}-\mathbf{v}_h|^2\, ds\Big)^{\frac{1}{2}}\\
&\le C\|\xi_{\mathbf{u}}\|_V h^{\frac{1}{2}} \|\mathbf{w}\|^{\frac{1}{2}}_{L^\infty(\Omega)} \|\mathbf{v}\|_{H^1(\Omega)}.
\end{aligned}$$

To estimate the second integral, we use the trace theorem for functions in $H^1(\Omega)$. This yields

$$\begin{aligned}
\Big|\int_{\Gamma_+} \mathbf{w}\cdot\mathbf{n}\xi_{\mathbf{u}}\cdot\mathbf{v}\, ds\Big| &\le \Big(\int_\Gamma |\mathbf{w}\cdot\mathbf{n}||\xi_{\mathbf{u}}|^2\, ds\Big)^{\frac{1}{2}} \Big(\int_\Gamma |\mathbf{w}\cdot\mathbf{n}||\mathbf{v}|^2\, ds\Big)^{\frac{1}{2}}\\
&\le C\|\xi_{\mathbf{u}}\|_V \|\mathbf{w}\|^{\frac{1}{2}}_{L^\infty(\Omega)} \|\mathbf{v}\|_{H^1(\Omega)}.
\end{aligned}$$

As a consequence, we see that

$$T_{4,3} \leq C\|\xi_{\mathbf{u}}\|_V \|\mathbf{v}\|_{H^1(\Omega)}.$$

Hence, from the above estimates, (4.35) and (4.37), we conclude that

$$|T_4| \leq C\|\xi_{\mathbf{u}}\|_V (\|\mathbf{v}_h\|_{1,h} + \|\mathbf{v}\|_{H^1(\Omega)}) \leq C\|\xi_{\mathbf{u}}\|_V.$$

From Lemma 4.6 (with $\varepsilon = 1$) and Theorem 4.8, we then obtain:

$$|T_4| \leq C\left(\mathcal{E}(\mathbf{u}, \mathbf{b}, p) + \mathcal{A}(\mathbf{u}) + |\!|\!|(\mathbf{b} - \mathbf{c}, p - q, r - s)|\!|\!|\right). \tag{4.42}$$

Combining the above results with the estimates for T_1, T_2, T_3 and T_4 yields

$$\|p - p_h\|_{L^2(\Omega)} \leq C\left(\mathcal{E}(\mathbf{u}, \mathbf{b}, p) + \mathcal{A}(\mathbf{u}) + \|\eta_{\mathbf{u}}\|_{1,h} + |\!|\!|(\mathbf{b} - \mathbf{c}, p - q, r - s)|\!|\!|\right),$$

as required. □

Finally, we bound the error in r.

PROPOSITION 4.10. *There is a constant $C > 0$ independent of the mesh size and ν such that*

$$\|r - r_h\|_S \leq C\big(\mathcal{E}(\mathbf{u}, \mathbf{b}, p) + \mathcal{A}(\mathbf{u}) + |\!|\!|(\mathbf{b} - \mathbf{c}, p - q, r - s)|\!|\!|\big),$$

for any $\mathbf{c} \in \mathbf{C}_h^c$, $q \in Q_h$ and $s \in S_h^c$.

Proof: Let $\mathbf{c} \in \mathbf{C}_h^c$, $q \in Q_h$ and $s \in S_h^c$. As before, we adopt the notation from (4.14). By the triangle inequality, we have

$$\|r - r_h\|_S \leq \|\eta_r\|_S + \|\xi_r\|_S.$$

To bound the term $\|\xi_r\|_S$, we decompose ξ_r into

$$\xi_r = \xi_r^c + \xi_r^\perp, \qquad \xi_r^c \in S_h^c,\ \xi_r^\perp \in S_h^\perp, \tag{4.43}$$

according to (3.1). Since s belongs to the conforming space S_h^c, we have

$$\xi_r^c = (s - r_h^c), \qquad \xi_r^\perp = -r_h^\perp. \tag{4.44}$$

By the triangle inequality and the norm-equivalence in Proposition 3.3, we have

$$\|\xi_r\|_S \leq \|\xi_r^c\|_S + \|r_h^\perp\|_S \leq \|\xi_r^c\|_S + C|r_h^\perp|_S. \tag{4.45}$$

The latter term can be bounded by Theorem 4.8:

$$|r_h^\perp|_S \leq C\big(\mathcal{E}(\mathbf{u}, \mathbf{b}, p) + \mathcal{A}(\mathbf{u}) + |\!|\!|(\mathbf{b} - \mathbf{c}, p - q, r - s)|\!|\!|\big). \tag{4.46}$$

To bound the former term, we use (4.2) and the inf-sup condition for D in Proposition 3.4. We obtain

$$C\|\xi_r^c\|_S \leq \sup_{\mathbf{c} \in \mathbf{C}_h^c} \frac{\widetilde{D}_h(\mathbf{c}, \xi_r^c)}{\|\mathbf{c}\|_C}. \tag{4.47}$$

Using (4.43) and (4.44), we write

$$\widetilde{D}_h(\mathbf{c}, \xi_r^c) = \widetilde{D}_h(\mathbf{c}, \eta_r + \xi_r) - \widetilde{D}_h(\mathbf{c}, \eta_r) + \widetilde{D}_h(\mathbf{c}, r_h^\perp),$$

and use the error equation (4.4) to conclude that

$$\begin{aligned}\widetilde{D}_h(\mathbf{c},\xi_r^c) = \mathcal{R}_M(\mathbf{c}) - \widetilde{M}_h(\eta_{\mathbf{b}},\mathbf{c}) + C_h(\eta_{\mathbf{u}},\mathbf{c})\\ -\widetilde{M}_h(\xi_{\mathbf{b}},\mathbf{c}) + C_h(\xi_{\mathbf{u}},\mathbf{c}) - \widetilde{D}_h(\mathbf{c},\eta_r) + D_h(\mathbf{c},r_h^\perp)\end{aligned}$$

for all $\mathbf{c} \in \mathbf{C}_h^c$. We note that $\mathcal{R}_M(\mathbf{c}) = 0$ for $\mathbf{c} \in \mathbf{C}_h^c$. From Proposition 4.3 and assumption (2.5), we have

$$\begin{aligned}C_h(\eta_{\mathbf{u}},\mathbf{c}) &\le C\|\eta_{\mathbf{u}}\|_\star|\mathbf{c}|_C,\\ C_h(\xi_{\mathbf{u}},\mathbf{c}) &\le C\|\xi_{\mathbf{u}}\|_{L^2(\Omega)}|\mathbf{c}|_C \le C\|\xi_{\mathbf{u}}\|_V|\mathbf{c}|_C.\end{aligned}$$

Using these estimates, the continuity properties in Proposition 4.1 and the norm-equivalence in Proposition 3.3, we obtain

$$\begin{aligned}|\widetilde{D}_h(\mathbf{c},\xi_r^c)| &\le C\|\mathbf{c}\|_C\big(|\eta_{\mathbf{b}}|_C + \|\eta_{\mathbf{u}}\|_\star + |\xi_{\mathbf{b}}|_C + \|\xi_{\mathbf{u}}\|_V + \|\eta_r\|_S + \|r_h^\perp\|_S\big)\\ &\le C\|\mathbf{c}\|_C\big(\|\eta_{\mathbf{b}}\|_C + \|\eta_{\mathbf{u}}\|_\star + \|\mathbf{b}-\mathbf{b}_h\|_C + \|\xi_{\mathbf{u}}\|_V + \|\eta_r\|_S + |r_h^\perp|_S\big).\end{aligned} \tag{4.48}$$

Referring to (4.45), (4.46), (4.47), (4.48), Lemma 4.6 (with $\varepsilon = 1$) and Theorem 4.8 shows

$$\begin{aligned}\|r-r_h\|_S &\le C\big(\mathcal{E}(\mathbf{u},\mathbf{b},p) + \mathcal{A}(\mathbf{u}) + \|\mathbf{b}-\mathbf{b}_h\|_C + |\!|\!|(\mathbf{b}-\mathbf{c},p-q,r-s)|\!|\!|\big)\\ &\le C\big(\mathcal{E}(\mathbf{u},\mathbf{b},p) + \mathcal{A}(\mathbf{u}) + |\!|\!|(\mathbf{b}-\mathbf{c},p-q,r-s)|\!|\!|\big).\end{aligned}$$

This completes the proof. □

4.3.3. Proof of Theorem 3.7. We are now ready to complete the proof of Theorem 3.7. In (4.11), the approximation for the velocity $\mathbf{u}$ has already be chosen to be the BDM projection $\mathbf{\Pi}_B\mathbf{u}$ of degree k. With this definition, the following result holds.

PROPOSITION 4.11. *Under the regularity assumptions in (3.5), there holds:*

$$\begin{aligned}\|\eta_{\mathbf{u}}\|_{1,h} &\le Ch^{\min\{\sigma,k\}}\|\mathbf{u}\|_{\sigma+1,\mathcal{T}_h},\\ \mathcal{O}(\mathbf{u}) &\le C\min\{1, v^{-\frac12}h + h^{\frac12}\}h^{\min\{\sigma,k\}}\|\mathbf{u}\|_{\sigma+1,\mathcal{T}_h},\\ \mathcal{A}(\mathbf{u}) &\le C(\nu^{\frac12} + \min\{1,\nu^{-\frac12}h + h^{\frac12}\})h^{\min\{\sigma,k\}}\|\mathbf{u}\|_{\sigma+1,\mathcal{T}_h},\end{aligned}$$

with constants $C > 0$ that are independent of the mesh size and ν.

Proof: The approximation properties of the BDM projection in [6, Proposition III.3.6] readily yield the first estimate of the proposition and also the following:

$$\begin{aligned}\|\eta_{\mathbf{u}}\|_O &\le C(\nu^{-\frac12}h + h^{\frac12})h^{\min\{\sigma,k\}+1}\|\mathbf{u}\|_{\sigma+1,\mathcal{T}_h},\\ \|\eta_{\mathbf{u}}\|_V &\le C\big(\nu^{\frac12} + \|\gamma_0\|_{L^\infty(\Omega)}^{\frac12}h + \|\mathbf{w}\|_{L^\infty(\Omega)}^{\frac12}h^{\frac12}\big)h^{\min\{\sigma,k\}}\|\mathbf{u}\|_{\sigma+1,\mathcal{T}_h},\\ \|\eta_{\mathbf{u}}\|_\star &\le Ch^{\min\{\sigma,k\}+1}\|\mathbf{u}\|_{\sigma+1,\mathcal{T}_h}.\end{aligned}$$

To bound $\mathcal{O}(\mathbf{u})$, we use the two continuity results in Proposition 4.4 to obtain that, for $\mathbf{v} \in \mathbf{V}_h$,

$$|O_h(\eta_{\mathbf{u}},\mathbf{v})| \le C\min\{\|\eta_{\mathbf{u}}\|_{1,h}, \|\eta_{\mathbf{u}}\|_O\}\|\mathbf{v}\|_V.$$

The estimates for $\|\eta_{\mathbf{u}}\|_{1,h}$ and $\|\eta_{\mathbf{u}}\|_O$ now imply the desired bound for $\mathcal{O}(\mathbf{u})$. The bound for $\mathcal{A}(\mathbf{u})$ is established similarly by noting that

$$\mathcal{A}(\mathbf{u}) \leq C \left(\|\eta_{\mathbf{u}}\|_V + \|\eta_{\mathbf{u}}\|_\star + \mathcal{O}(\mathbf{u}) \right).$$

This completes the proof. □

We now approximate the remaining fields as follows:

$$\mathbf{c} = \mathbf{\Pi}_N \mathbf{b}, \qquad q = \Pi_{k-1} p, \qquad s = \Pi_S r, \tag{4.49}$$

where $\mathbf{\Pi}_N$ is the $H(\mathrm{curl};\Omega)$-conforming Nédélec projection of the second kind of degree k onto $\mathbf{C}_h^c$; see [33]. Its approximation properties are listed in [32, Theorem 8.15 and Remark 5.42]. Moreover, Π_{k-1} is the L^2-projection of degree $k-1$ onto Q_h, and Π_S is the standard H^1-conforming nodal interpolation operator of degree $k+1$ into S_h, cf. [32, Theorem 5.48].

The approximation properties of these operators immediately yield the following result.

PROPOSITION 4.12. *Assume the smoothness properties (3.5) and (3.6). Choosing the interpolants as in (4.49), there holds*

$$\begin{aligned} |\!|\!| (\mathbf{b}-\mathbf{c}, p-q, r-s) |\!|\!| \leq & C \nu^{-\frac{1}{2}} h^{\min\{\sigma,k\}} \|p\|_{\sigma,\mathcal{T}_h} \\ & + C h^{\min\{\tau,k\}} \left(\|\mathbf{b}\|_{\tau,\mathcal{T}_h} + \|\nabla \times \mathbf{b}\|_{\tau,\mathcal{T}_h} + \|r\|_{\tau+1,\mathcal{T}_h} \right), \end{aligned}$$

with constants $C > 0$ that are independent of the mesh size and ν.

The error estimate in Theorem 3.7 follows now directly from the error estimates in Theorem 4.8, Proposition 4.9 and Proposition 4.10, in conjunction with the approximation results in Proposition 4.2, Proposition 4.11 and Proposition 4.12.

5. Numerical Results. In this section we present a series of numerical experiments to highlight the practical performance of the mixed DG method introduced in this article for the numerical approximation of incompressible MHD problems. To confirm the convergence rates predicted by our analysis, we consider two problems with smooth solutions and a third one with a singular solution. Finally, we consider the numerical approximation of both two– and three–dimensional Hartmann channel flow problems. Throughout this section, we select the stabilization parameters as follows:

$$a_0 = \alpha\, k^2, \quad m_0 = \mu\, k^2 \quad \text{and} \quad s_0 = 1,$$

$\alpha, \mu > 0$, cf. [28], for example. To ensure stability of the underlying DG method we set $\alpha = \mu = 10$ in two dimensions; for three-dimensional simulations, it is necessary to increase α and μ to $\alpha = \mu = 20$.

5.1. Smooth solutions. First, we verify the theoretical error bound stated in Theorem 3.7 for problems with smooth analytical solutions.

5.1.1. Example 1: A two-dimensional problem in an L–shaped domain. The first example we consider is a two-dimensional version of the MHD problem (2.1)–(2.4). While the Navier-Stokes operator has the same form in two dimensions, some care is required for the curl-curl operator and the coupling terms in the equations; see also [32, Page 51]. For a two-dimensional vector $\mathbf{b} = (b_1, b_2)$, the curl of $\mathbf{b}$ is defined as the scalar quantity $\nabla \times \mathbf{b} = \partial_x b_2 - \partial_y b_1$; meanwhile for a scalar function b, we

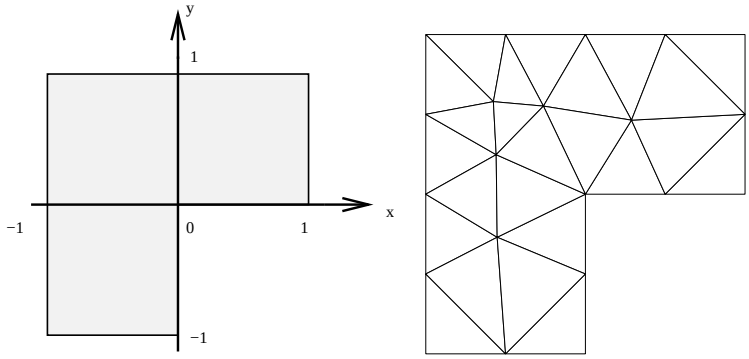

FIG. 5.1. *Example 1. (a) Problem domain; (b) Initial unstructured triangular mesh.*

define its vector curl as $\nabla \times b = (\partial_y b, -\partial_x b)$. Furthermore, the cross product of two vectors is defined as $\mathbf{a} \times \mathbf{b} = a_1 b_2 - a_2 b_1$; while the cross product of a scalar and a vector is $a \times \mathbf{b} = (-ab_2, ab_1)$. With this notation, the DG method can then be straightforwardly extended to the two-dimensional variant of (2.1)–(2.4).

We consider the L–shaped domain $\Omega = (-1,1)^2 \setminus ([0,1) \times (-1,0])$ with $\Gamma_N = \{(1,y) : y \in (0,1)\}$ and $\Gamma_D = \partial\Omega \setminus \Gamma_N$, cf. Figure 5.1(a). We set $\nu = \nu_m = \kappa = 1$, $\mathbf{w} = (2,1)$, $\gamma = 0$, $\mathbf{d} = (x,-y)$, and choose the forcing functions $\mathbf{f}$ and $\mathbf{g}$ and boundary conditions so that the analytical solution of the two-dimensional variant of (2.1)–(2.4) is of the form

$$\mathbf{u}(x,y) = (-(y\cos y + \sin y)\mathrm{e}^x, y\sin y\,\mathrm{e}^x), \qquad p(x,y) = 2\mathrm{e}^x \sin y,$$
$$\mathbf{b}(x,y) = (-(y\cos y + \sin y)\mathrm{e}^x, y\sin y\,\mathrm{e}^x), \qquad r(x,y) = -\sin \pi x \, \sin \pi y.$$

Here, we investigate the asymptotic convergence of the interior penalty DG method (2.21)–(2.24) on a sequence of successively finer quasi-uniform unstructured triangular meshes for $k = 1,2,3,4$. In each case the meshes are constructed by uniformly refining the initial unstructured mesh depicted in Figure 5.1(b).

In Figure 5.2 we plot the norms $\|\cdot\|_V$, $\|\cdot\|_C$, and $\|\cdot\|_S$ of the errors $\mathbf{u} - \mathbf{u}_h$, $\mathbf{b} - \mathbf{b}_h$, and $r - r_h$, respectively, against the square root of the number of degrees of freedom in the finite element space $\mathbf{V}_h \times \mathbf{C}_h \times Q_h \times S_h$. Here, we observe that both $\|\mathbf{u} - \mathbf{u}_h\|_V$ and $\|\mathbf{b} - \mathbf{b}_h\|_C$ converge to zero, for each fixed k, at the optimal rate $\mathcal{O}(h^k)$, as the mesh is refined, in accordance with Theorem 3.7. On the other hand, for this mixed-order method, $\|r - r_h\|_S$ converges at the rate $\mathcal{O}(h^{k+1})$, for each k, as h tends to zero; this rate is indeed optimal, though this is not reflected by Theorem 3.7, cf. also [28]. Additionally, in Figure 5.2(d), we plot the sum of the three error contributions with respect to the square root of the number of degrees of freedom in the finite element space. Clearly, as above, this converges to zero at the optimal rate predicted by Theorem 3.7.

Secondly, we highlight the optimality of the proposed mixed method when the components of the error are measured in terms of the L^2-norm. From Figure 5.3 we observe that the L^2-norm of the error in both the approximation to the velocity field $\mathbf{u}$ and the magnetic field $\mathbf{b}$ tend to zero at the expected optimal rate $\mathcal{O}(h^{k+1})$, for each k, as h tends to zero. In agreement with Theorem 3.7, for each fixed k, the L^2-norm of the error in the pressure p tends to zero at the optimal rate $\mathcal{O}(h^k)$ as the mesh is enriched, while $\|r - r_h\|_{L^2(\Omega)}$ is of order $\mathcal{O}(h^{k+2})$ as h tends to zero.

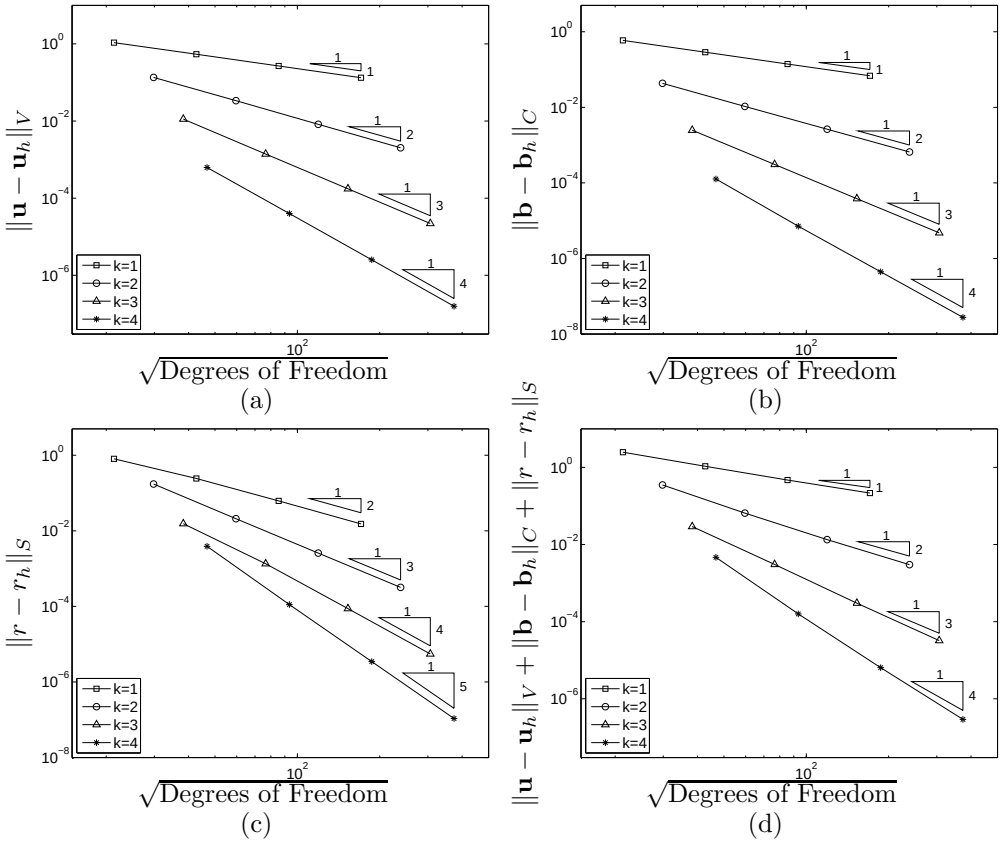

FIG. 5.2. *Example 1. Convergence with h-refinement: (a)* $\|\mathbf{u}-\mathbf{u}_h\|_V$*; (b)* $\|\mathbf{b}-\mathbf{b}_h\|_C$*; (c)* $\|r-r_h\|_S$*; (d)* $\|\mathbf{u}-\mathbf{u}_h\|_V+\|\mathbf{b}-\mathbf{b}_h\|_C+\|r-r_h\|_S$.

5.1.2. Example 2: A three-dimensional problem in the unit cube. The second example is a 3D problem with a smooth analytical solution. To this end, we set $\Omega=(0,1)^3\subset\mathbb{R}^3$ with $\Gamma_D=\partial\Omega$ and $\Gamma_N=\emptyset$. Furthermore, we set $\nu=\nu_m=\kappa=1$, $\mathbf{w}=(2,1,1)$, $\gamma=0$, and $\mathbf{d}=(x,-y,1)$, and select $\mathbf{f}$ and $\mathbf{g}$, together with appropriate inhomogeneous boundary conditions, so that the solution of the incompressible MHD system (2.1)–(2.4) is given by

$$\begin{aligned}
\mathbf{u}&=(-(y\cos y+\sin y+z\cos z)\mathrm{e}^x, y\sin y\,\mathrm{e}^x, z\sin z\,\mathrm{e}^x),\\
\mathbf{b}&=(-(y\cos y+\sin y+z\cos(z))\mathrm{e}^x, y\sin y\,\mathrm{e}^x, z\sin z\,\mathrm{e}^x),\\
p&=2\mathrm{e}^x(\sin y+\sin z)-p_0,\qquad r=\sin\pi x\,\sin\pi y\,\sin\pi z,
\end{aligned}$$

where $p_0=4(-1+\mathrm{e}+\cos 1-\mathrm{e}\cos 1)$.

In Table 5.1 we investigate the asymptotic rate of convergence of the error in the approximation of the hydrodynamic variables; here, l denotes the computed rate of convergence. To this end, we show $\|\mathbf{u}-\mathbf{u}_h\|_{L^2(\Omega)}$, $\|\mathbf{u}-\mathbf{u}_h\|_V$, and $\|p-p_h\|_{L^2(\Omega)}$ computed on a sequence of uniformly refined tetrahedral meshes for $k=1,2$. As in the previous example, we again observe optimal rates of convergence for all three measures of the error. Indeed, in accordance with Theorem 3.7, both $\|\mathbf{u}-\mathbf{u}_h\|_V$ and $\|p-p_h\|_{L^2(\Omega)}$ tend to zero at the optimal rate $\mathcal{O}(h^k)$, for each fixed k, as the mesh

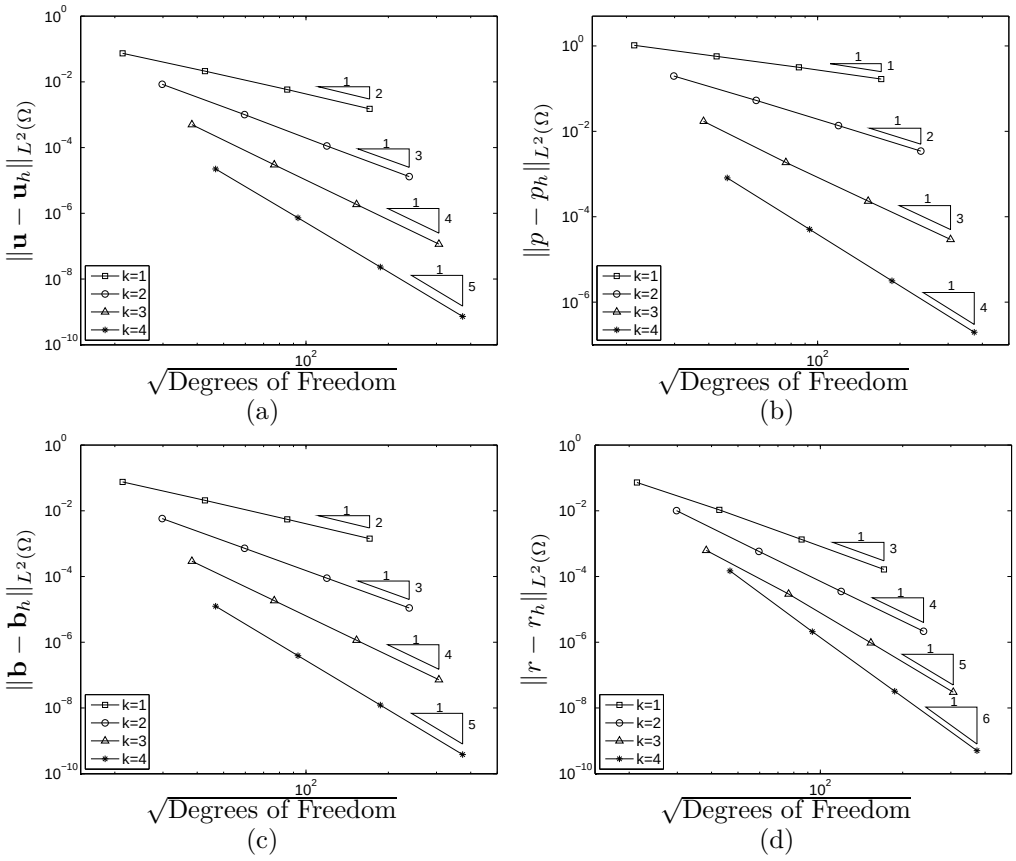

FIG. 5.3. *Example 1. Convergence with h-refinement: (a)* $\|\mathbf{u}-\mathbf{u}_h\|_{L^2(\Omega)}$*; (b)* $\|p-p_h\|_{L^2(\Omega)}$*; (c)* $\|\mathbf{b}-\mathbf{b}_h\|_{L^2(\Omega)}$*; (d)* $\|r-r_h\|_{L^2(\Omega)}$*.*

k	DOFs in $\mathbf{u_h}/p_h$	$\|\mathbf{u}-\mathbf{u}_h\|_{L^2(\Omega)}$	l	$\|\mathbf{u}-\mathbf{u}_h\|_V$	l	$\|p-p_h\|_{L^2(\Omega)}$	l
	576/48	6.400e-2	–	1.168	–	7.321e-1	–
1	4608/384	1.647e-2	1.96	5.823e-1	1.00	4.564e-1	0.68
	36864/3072	4.213e-3	1.97	2.896e-1	1.01	2.606e-1	0.81
	294912/24576	1.072e-3	1.97	1.442e-1	1.01	1.400e-1	0.90
	1440/192	5.082e-3	–	1.262e-1	–	3.424e-1	–
2	11520/1536	6.802e-4	2.90	3.162e-2	2.00	8.488e-2	2.01
	92160/12288	8.417e-5	3.01	7.822e-3	2.02	2.127e-2	2.00

TABLE 5.1

Example 2: Convergence of $\|\mathbf{u}-\mathbf{u}_h\|_{L^2(\Omega)}$*,* $\|\mathbf{u}-\mathbf{u}_h\|_V$*, and* $\|p-p_h\|_{L^2(\Omega)}$ *with h-refinement.*

is refined. Additionally, we observe that the L^2-norm of the error in the velocity is of optimal order $\mathcal{O}(h^{k+1})$ as h tends to zero.

The corresponding errors for the magnetic variables are shown in Tables 5.2 & 5.3. Here, we clearly observe the optimality of the approximation to the magnetic field $\mathbf{b}$. Indeed, from Table 5.2 we observe that $\|\mathbf{b}-\mathbf{b}_h\|_{L^2(\Omega)}$ and $\|\mathbf{b}-\mathbf{b}_h\|_C$ converge to zero at the optimal rates $\mathcal{O}(h^{k+1})$ and $\mathcal{O}(h^k)$, respectively, for each fixed k, as the

k	DOFs in $\mathbf{b}_h$	$\|\mathbf{b}-\mathbf{b}_h\|_{L^2(\Omega)}$	l	$\|\mathbf{b}-\mathbf{b}_h\|_C$	l
	576	7.289e-2	–	7.324e-1	–
1	4608	2.076e-2	1.81	3.445e-1	1.09
	36864	5.486e-3	1.92	1.668e-1	1.05
	294912	1.399e-3	1.97	8.184e-2	1.03
	1440	6.082e-3	–	4.920e-2	–
2	11520	7.953e-4	2.94	1.146e-2	2.10
	92160	1.006e-4	2.98	2.767e-3	2.05

TABLE 5.2

Example 2: Convergence of $\|\mathbf{b}-\mathbf{b}_h\|_{L^2(\Omega)}$ and $\|\mathbf{b}-\mathbf{b}_h\|_C$ with h-refinement.

k	DOFs in r_h	$\|r-r_h\|_{L^2(\Omega)}$	l	$\|r-r_h\|_S$	l
	480	1.038e-1	–	1.546	–
1	3840	1.766e-2	2.56	5.098e-1	1.60
	30720	2.350e-3	2.91	1.363e-1	1.90
	245760	2.924e-4	3.01	3.405e-2	2.00
	960	1.327e-2	–	2.559e-1	–
2	7680	8.567e-4	3.95	3.430e-2	2.90
	61440	5.135e-5	4.06	4.210e-3	3.03

TABLE 5.3

Example 2: Convergence of $\|r-r_h\|_{L^2(\Omega)}$ and $\|r-r_h\|_S$ with h-refinement.

mesh is refined. As in the previous (two–dimensional) example, we again observe that $\|r-r_h\|_{L^2(\Omega)}$ and $\|r-r_h\|_S$ are of order $\mathcal{O}(h^{k+2})$ and $\mathcal{O}(h^{k+1})$, respectively, as the mesh is uniformly refined.

5.2. Example 3: A two-dimensional problem with a singular solution. To verify the ability of the proposed interior penalty DG method to capture the strongest magnetic (and hydrodynamic) singularities, we consider a problem in which the precise regularity of the analytical solution is known. To this end, we again let Ω be the L-shaped domain employed in Example 1 above with $\Gamma_N = \{(1,y) : y \in (0,1)\}$ and $\Gamma_D = \partial\Omega \setminus \Gamma_N$. We choose $\nu = \nu_m = \kappa = 1$, and set $\mathbf{w} = \mathbf{0}$, $\gamma = 0$ and $\mathbf{d} = (-1,1)$. Hence, the Navier-Stokes operator coincides with the Stokes equations. We further choose $\mathbf{f}$ and $\mathbf{g}$, and appropriate inhomogeneous boundary conditions so that the solution to this problem is given by the strongest corner singularities for the underlying elliptic operators. That is, in polar coordinates (ρ,ϕ) around the origin, the hydrodynamic solution components $\mathbf{u}$ and p are taken to be

$$\mathbf{u}(\rho,\phi) = \begin{bmatrix} \rho^\lambda((1+\lambda)\sin(\phi)\psi(\phi) + \cos(\phi)\psi'(\phi)) \\ \rho^\lambda(-(1+\lambda)\cos(\phi)\psi(\phi) + \sin(\phi)\psi'(\phi)) \end{bmatrix},$$

$$p(\rho,\phi) = -\rho^{\lambda-1}((1+\lambda)^2\psi'(\phi) + \psi'''(\phi))/(1-\lambda),$$

where

$$\begin{aligned}\psi(\phi) =& \sin((1+\lambda)\phi)\cos(\lambda w)/(1+\lambda) - \cos((1+\lambda)\phi) \\ & - \sin((1-\lambda)\phi)\cos(\lambda w)/(1-\lambda) + \cos((1-\lambda)\phi),\end{aligned}$$

k	DOFs in $\mathbf{u_h}/p_h$	$\|\mathbf{u}-\mathbf{u}_h\|_{L^2(\Omega)}$	l	$\|\mathbf{u}-\mathbf{u}_h\|_V$	l	$\|p-p_h\|_{L^2(\Omega)}$	l
1	144/24	1.311e-1	–	1.910	–	1.443	–
	576/96	4.638e-2	1.50	1.352	0.50	1.064	0.44
	2304/384	1.632e-2	1.51	9.419e-1	0.52	7.690e-1	0.47
	9216/1536	5.837e-3	1.48	6.510e-1	0.53	5.436e-1	0.50
	36864/6144	2.120e-3	1.46	4.482e-1	0.54	3.789e-1	0.52
2	288/72	6.089e-2	–	1.075	–	1.520	–
	1152/288	2.405e-2	1.34	7.382e-1	0.54	9.010e-1	0.75
	4608/1152	9.434e-3	1.35	5.065e-1	0.54	5.852e-1	0.62
	18432/4608	3.837e-3	1.30	3.474e-1	0.54	3.910e-1	0.58
	73728/18432	1.630e-3	1.24	2.383e-1	0.54	2.649e-1	0.56
3	480/144	3.094e-2	–	7.498e-1	–	9.219e-1	–
	1920/576	1.198e-2	1.37	5.151e-1	0.54	5.809e-1	0.67
	7680/2304	4.844e-3	1.31	3.532e-1	0.54	3.779e-1	0.62
	30720/9216	2.054e-3	1.24	2.422e-1	0.54	2.527e-1	0.58
	122880/36864	9.046e-4	1.18	1.661e-1	0.54	1.713e-1	0.56

TABLE 5.4

Example 3: Convergence of $\|\mathbf{u}-\mathbf{u}_h\|_{L^2(\Omega)}$, $\|\mathbf{u}-\mathbf{u}_h\|_V$, and $\|p-p_h\|_{L^2(\Omega)}$ with h-refinement.

and $\lambda \approx 0.54448373678246$. The magnetic pair $(\mathbf{b}, r)$ is taken as

$$\mathbf{b}(\mathbf{x}) = \nabla(\rho^{2/3}\sin(2/3\phi)), \qquad r(\mathbf{x}) \equiv 0.$$

We point out that the magnetic field $\mathbf{b}$ does not belong to $H^1(\Omega)^2$ and thus cannot be correctly captured by nodal elements. In fact, for this example, we have that $(\mathbf{u}, p) \in H^{1+\lambda}(\Omega)^2 \times H^{\lambda}(\Omega)$ and $\mathbf{b} \in H^{2/3}(\Omega)^2$. Thus, the limiting regularity exponent, cf. (3.5) and (3.6), appearing in Theorem 3.7 is λ which stems from the regularity of the hydrodynamic variables.

In this example we study the asymptotic convergence of the interior penalty DG method (2.21)–(2.24) on the sequence of successively finer quasi-uniform unstructured triangular meshes employed in Example 1, cf. Figure 5.1(b) for the initial mesh, with $k = 1, 2, 3$. Table 5.4 presents the L^2-norm of the error in both the computed velocity $\mathbf{u}_h$ and pressure p_h, as well as the $\|\cdot\|_V$-norm of the error in $\mathbf{u}_h$. In agreement with Theorem 3.7 we see that both $\|\mathbf{u}-\mathbf{u}_h\|_V$ and $\|p-p_h\|_{L^2(\Omega)}$ tend to zero at the optimal rate $\mathcal{O}(h^{\lambda})$ as h tends to zero. The rate of convergence of $\|\mathbf{u}-\mathbf{u}_h\|_{L^2(\Omega)}$ is observed to be between $\mathcal{O}(h^{1.2})$ and $\mathcal{O}(h^{1.5})$ approximately as the mesh is uniformly refined.

From Table 5.5 we observe that both $\|\mathbf{b}-\mathbf{b}_h\|_{L^2(\Omega)}$ and $\|\mathbf{b}-\mathbf{b}_h\|_C$ are approximately $\mathcal{O}(h)$ as h tends to zero. For this latter error, this rate is higher than what we would expect from Theorem 3.7. However, this same behavior of the error has also been observed in the case of simply approximating the time-harmonic Maxwell operator in isolation, cf. [28], for example. In contrast, from Table 5.6, we observe that $\|r-r_h\|_S$ converges to zero at the rate $\mathcal{O}(h^{2/3})$ as the mesh is refined. In terms of the numerical approximation of the time-harmonic Maxwell operator in isolation, this rate is indeed optimal, cf. [28], though this is not reflected in Theorem 3.7. Finally, we note that the L^2-norm of the error in the approximation to the Lagrange multiplier variable r tends to zero at the rate $\mathcal{O}(h^{4/3})$ as h tends to zero.

5.3. Hartmann channel flow. Finally, we consider the Hartmann channel flow problems in two and three dimensions; cf. [20].

k	DOFs in $\mathbf{b}_h$	$\|\mathbf{b}-\mathbf{b}_h\|_{L^2(\Omega)}$	l	$\|\mathbf{b}-\mathbf{b}_h\|_C$	l
	144	2.601e-1	–	4.091e-1	–
	576	1.492e-1	0.80	2.291e-1	0.84
1	2304	7.699e-2	0.96	1.112e-1	1.04
	9216	4.038e-2	0.93	5.280e-2	1.07
	36864	2.265e-2	0.84	2.657e-2	0.99
	288	2.244e-1	–	3.649e-1	–
	1152	1.124e-1	1.00	1.785e-1	1.03
2	4608	5.371e-2	1.07	8.065e-2	1.15
	18432	2.679e-2	1.00	3.654e-2	1.14
	73728	1.452e-2	0.88	1.766e-2	1.05
	480	1.888e-1	–	3.090e-1	–
	1920	9.013e-2	1.07	1.448e-2	1.09
3	7680	4.156e-2	1.12	6.363e-2	1.19
	30720	2.004e-2	1.05	2.812e-2	1.18
	122880	1.055e-2	0.93	1.320e-2	1.09

TABLE 5.5
Example 3: Convergence of $\|\mathbf{b}-\mathbf{b}_h\|_{L^2(\Omega)}$ and $\|\mathbf{b}-\mathbf{b}_h\|_C$ with h-refinement.

k	DOFs in r_h	$\|r-r_h\|_{L^2(\Omega)}$	l	$\|r-r_h\|_S$	l
	144	2.397e-1	–	2.107	–
	576	1.150e-1	1.06	1.768	0.25
1	2304	4.860e-2	1.24	1.265	0.48
	9216	1.946e-2	1.32	8.384e-1	0.59
	36864	7.664e-3	1.34	5.387e-1	0.64
	240	1.944e-1	–	2.728	–
	960	8.588e-2	1.18	2.066	0.40
2	3840	3.498e-2	1.30	1.412	0.55
	15360	1.382e-2	1.34	9.193e-1	0.62
	61440	5.419e-3	1.35	5.868e-1	0.65
	360	1.621e-1	–	3.188	–
	1440	6.932e-2	1.23	2.323	0.46
3	5760	2.784e-2	1.32	1.559	0.58
	23040	1.095e-2	1.35	1.008	0.63
	92160	4.290e-3	1.35	6.415e-1	0.65

TABLE 5.6
Example 3: Convergence of $\|r-r_h\|_{L^2(\Omega)}$ and $\|r-r_h\|_S$ with h-refinement.

5.3.1. Example 4: Two-dimensional Hartmann flow. In the domain $\Omega = (0,L)\times(-1,1)$, $L \gg 1$, we consider the steady one-dimensional unidirectional flow under a constant pressure gradient $-G$ in the x–direction, where theoretically G can be any real number, and practically any achievable pressure change produced by external forces. We set

$$\mathbf{w} = \left(\frac{G}{\nu \mathrm{Ha}\tanh(\mathrm{Ha})}\left(1-\frac{\cosh(y\mathrm{Ha})}{\cosh(\mathrm{Ha})}\right),0\right), \qquad \mathbf{d} = \left(\frac{G}{\kappa}\left(\frac{\sinh(y\mathrm{Ha})}{\sinh(\mathrm{Ha})}-y\right),1\right),$$

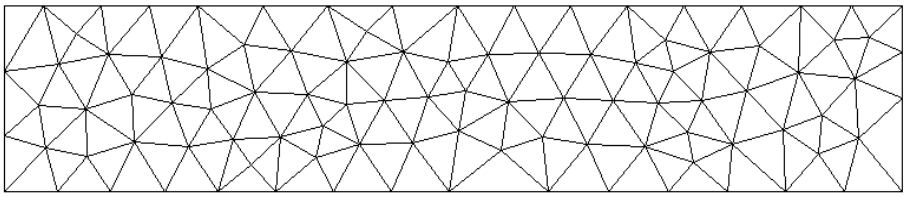

FIG. 5.4. *Example 4. Initial unstructured triangular mesh.*

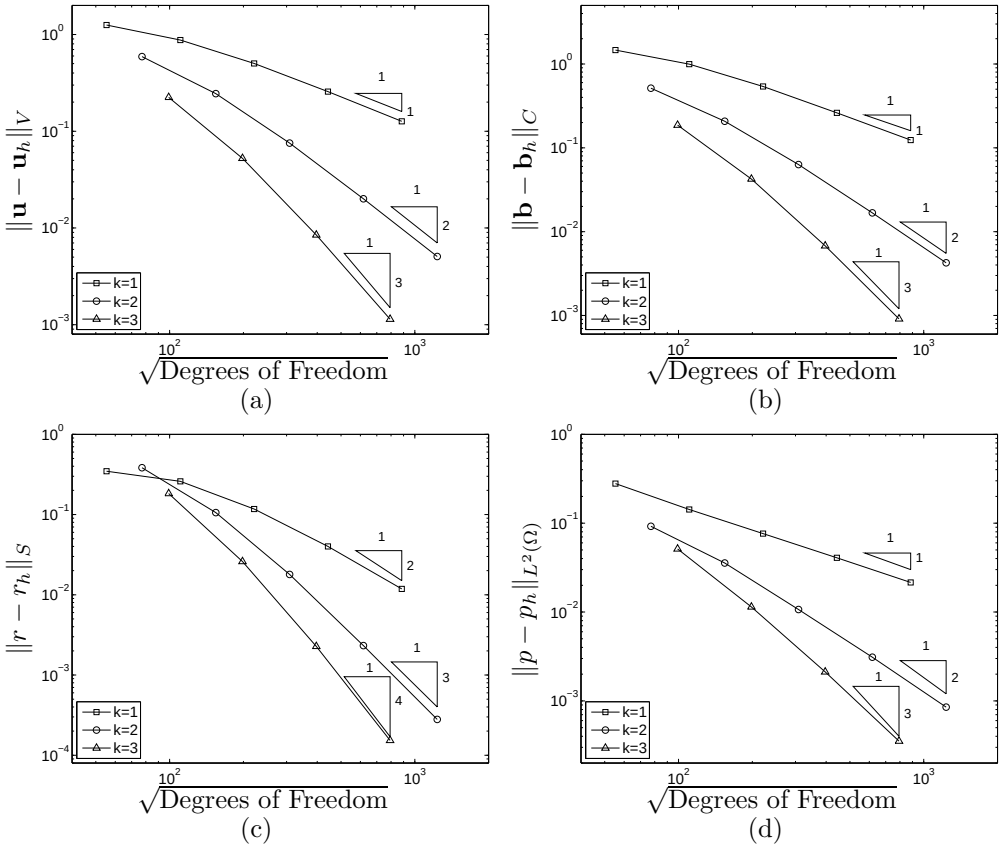

FIG. 5.5. *Example 4. Convergence with h-refinement: (a) $\|\mathbf{u}-\mathbf{u}_h\|_V$; (b) $\|\mathbf{b}-\mathbf{b}_h\|_C$; (c) $\|r-r_h\|_S$; (d) $\|p-p_h\|_{L^2(\Omega)}$.*

$\gamma = 0$, $\mathbf{f} = \mathbf{0}$, and $\mathbf{g} = \mathbf{0}$. Additionally, we impose the boundary conditions

$$\begin{aligned} \mathbf{u} &= \mathbf{0} && \text{on } y = \pm 1, \\ p\mathbf{n} &= p_N \mathbf{n} && \text{on } x = 0 \text{ and } x = L, \\ \mathbf{n} \times \mathbf{b} &= \mathbf{n} \times \mathbf{b}_D && \text{on } \Gamma, \end{aligned}$$

where

$$\mathbf{b}_D = (0, 1), \qquad p_N = -Gx - \frac{G^2}{2\kappa}\left(\frac{\sinh(y\mathrm{Ha})}{\sinh(\mathrm{Ha})} - y\right)^2 + p_0,$$

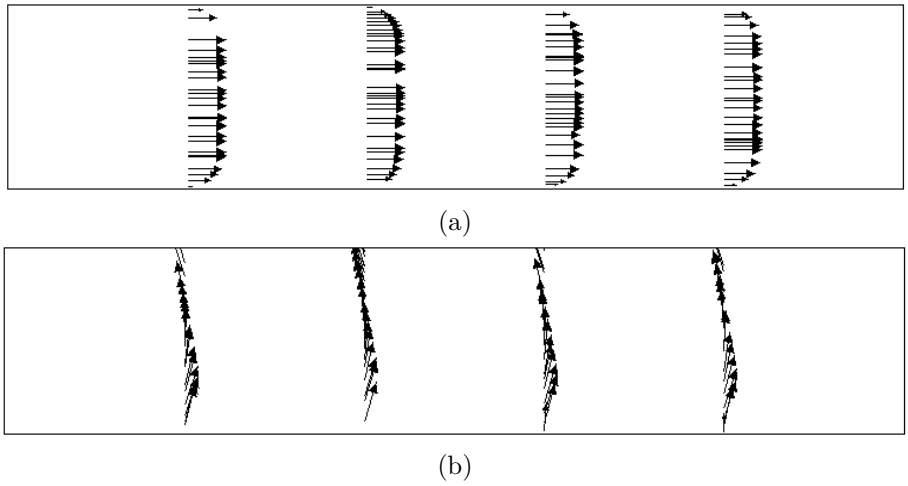

FIG. 5.6. *Example 4. DG solution computed on the finest mesh with $k = 1$: (a) Velocity field; (b) Magnetic field.*

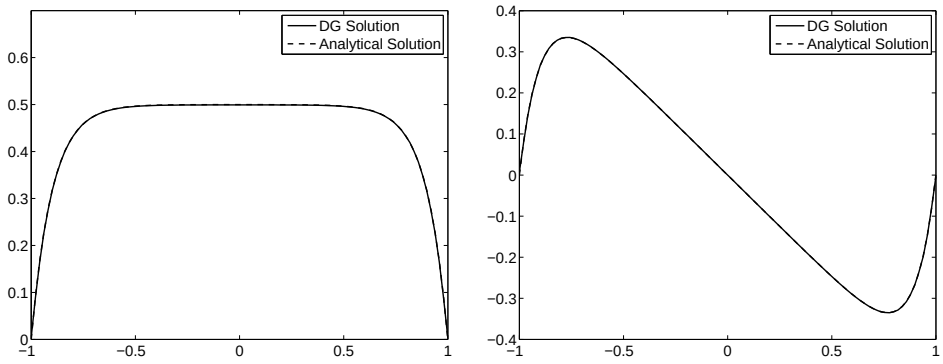

FIG. 5.7. *Example 4. DG solution computed on the finest mesh with $k = 1$. Slices along $x = 5$, $-1 \leq y \leq 1$ of the solution: (a) First component of the velocity field; (b) First component of the magnetic field.*

and p_0 is any constant.

The analytical solution to the incompressible MHD equations is then given by

$$\mathbf{u} = \mathbf{w}, \qquad \mathbf{b} = \mathbf{d}, \qquad p = p_N, \qquad r \equiv 0, \tag{5.1}$$

where $\kappa = \nu\nu_m \mathrm{Ha}^2$. We note that the fluid always moves in the direction in which the pressure decreases. In this section we set $L = 10$, $\nu = \nu_m = 0.1$, $\mathrm{Ha} = 10$, $G = 0.5$, and $p_0 = 10$.

Firstly, in Figure 5.5 we investigate the asymptotic convergence of the interior penalty DG method (2.21)–(2.24) on a sequence of successively finer quasi-uniform unstructured triangular meshes for $k = 1, 2, 3$. In each case the meshes are constructed by uniformly refining the initial unstructured mesh depicted in Figure 5.4. Here, we plot the norms $\|\cdot\|_V$, $\|\cdot\|_C$, $\|\cdot\|_S$, and $\|\cdot\|_{L^2(\Omega)}$ of the errors $\mathbf{u} - \mathbf{u}_h$, $\mathbf{b} - \mathbf{b}_h$, $r - r_h$, and $p - p_h$, respectively, with respect to the square root of the number of degrees of

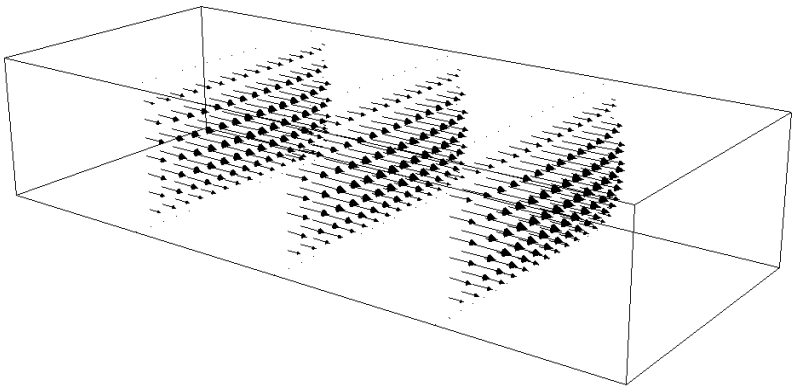

(a)

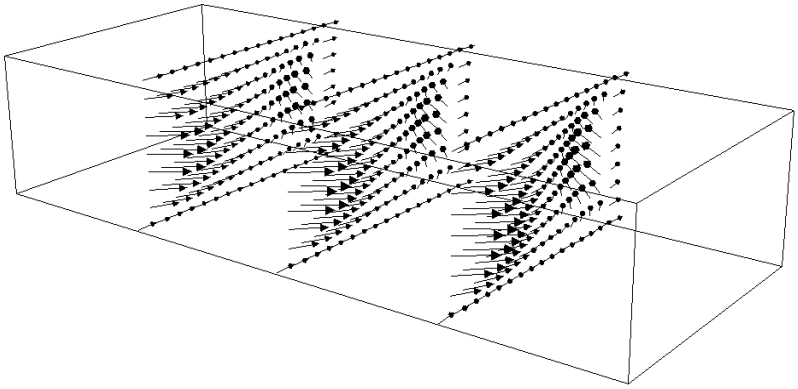

(b)

FIG. 5.8. *Example 5. DG solution computed on a uniform tetrahedral mesh with $k = 1$: (a) Velocity field; (b) Magnetic field.*

freedom in the finite element space $\mathbf{V}_h \times \mathbf{C}_h \times Q_h \times S_h$. As in the previous examples presented in Section 5.1, we observe that $\|\mathbf{u} - \mathbf{u}_h\|_V$, $\|\mathbf{b} - \mathbf{b}_h\|_C$ and $\|p - p_h\|_{L^2(\Omega)}$ converge to zero, for each fixed k, at the optimal rate $\mathcal{O}(h^k)$ as the mesh is refined, in accordance with Theorem 3.7, while $\|r - r_h\|_S$ converges at the rate $\mathcal{O}(h^{k+1})$, for each k, as h tends to zero. Moreover, we note that the L^2-norms of the error in the approximation to $\mathbf{u}$, $\mathbf{b}$ and r tend to zero optimally, cf. Section 5.1; for brevity, these results have been omitted.

Finally, in Figures 5.6 & 5.7 we show the DG solution computed on the finest mesh with 41216 elements, employing $k = 1$; thereby, the total number of degrees of freedom employed in the finite element space $\mathbf{V}_h \times \mathbf{C}_h \times Q_h \times S_h$ is 783104. In particular, from Figure 5.7, we observe extremely good agreement between the computed and analytical solutions of the first components in the velocity and magnetic fields.

5.3.2. Example 5: Three-dimensional Hartmann flow. In this final example, we consider the steady three-dimensional unidirectional flow in the rectangular duct given by $\Omega = [0, L] \times [-y_0, y_0] \times [-z_0, z_0]$ with $y_0, z_0 \ll L$. We take $\mathbf{w} = \mathbf{u}$ (cf. below), $\mathbf{f} = \mathbf{g} = \mathbf{0}$, $\gamma = 0$, $\mathbf{d} = (0, 1, 0)$, and consider solutions of the form

$$\mathbf{u} = (u(y, z), 0, 0), \qquad \mathbf{b} = (b(y, z), 1, 0), \qquad p = -Gx + p_0, \qquad r \equiv 0. \tag{5.2}$$

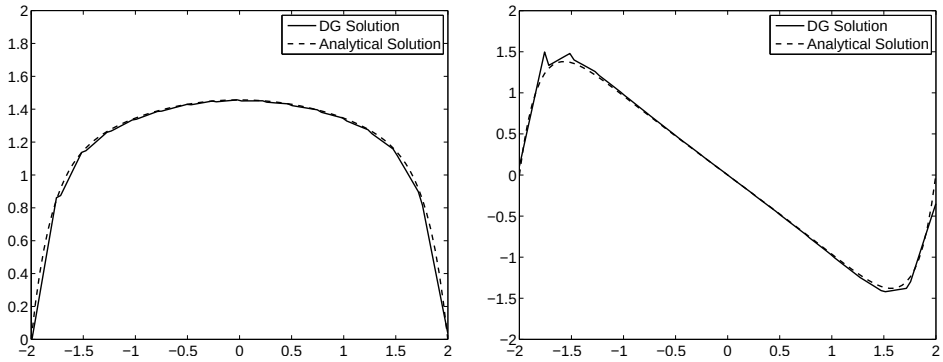

(a) (b)

FIG. 5.9. *Example 5. DG solution computed on a uniform tetrahedral mesh with $k = 1$. Slices along $x = 5$, $-1 \leq y \leq 1$, $z = 0$, of the solution: (a) First component of the velocity field; (b) First component of the magnetic field.*

We enforce the boundary conditions

$$\begin{aligned} \mathbf{u} &= \mathbf{0} && \text{for } y = \pm y_0 \text{ and } z = \pm z_0, \\ p\mathbf{n} &= p_N \mathbf{n} && \text{for } x = 0 \text{ and } x = L, \\ \mathbf{n} \times \mathbf{b} &= \mathbf{n} \times \mathbf{b}_D && \text{on } \Gamma, \end{aligned}$$

with $p_N = -Gx + p_0$ and $\mathbf{b}_D = (0, 1, 0)$. As before, G and p_0 are arbitrary constants. For this channel problem, the analytical solution can be expressed by Fourier series; for details, we refer to [18]. Throughout this section, we set $L = 10$, $y_0 = 2$, $z_0 = 1$, $\nu = \nu_m = 0.1$, Ha $= 5$, $G = 0.5$, and $p_0 = 10$.

In Figures 5.8 & 5.9 we show the DG solution computed on a uniform tetrahedral mesh comprising of 30720 elements with the polynomial degree $k = 1$; this results in a total of 1075200 degrees of freedom in the finite element space $\mathbf{V}_h \times \mathbf{C}_h \times Q_h \times S_h$. In particular, from Figure 5.9, we observe that there is reasonably good agreement between the computed and analytical solutions of the first components in the velocity and magnetic fields on this relatively coarse mesh. However, here we do observe some over-shoots in the computed solution, which are particularly evident in the approximation to the magnetic field.

6. Conclusions. In this paper, we have proposed and analyzed a discontinuous Galerkin method for a linear incompressible magnetohydrodynamics problem. The method is based on an interior penalty discretization of the mixed variational formulation proposed in [35]. We have derived a-priori error estimates and verified them in a set of numerical examples. We have further tested the methods for channel flow problems in both two- and three-dimensions.

We point out that the method and its analysis can be readily extended to other types of electromagnetic boundary conditions. Indeed, with only minimal changes, it is also possible to specify both $\mathbf{b}\cdot\mathbf{n}$ and $\nabla\times\mathbf{b}\times\mathbf{n}$ on Γ; see also [35]. Since we use BDM projections for the approximation of the velocity, our analysis immediately extends to the divergence-conforming $\mathcal{P}_k^3 - \mathcal{P}_{k-1}$ element proposed in [10]. This element yields an exactly divergence-free velocity approximation.

Ongoing work includes extensions of the method to fully nonlinear incompressible magnetohydrodynamics problems.

REFERENCES

[1] C. Amrouche, C. Bernardi, M. Dauge, and V. Girault. Vector potentials in three-dimensional non-smooth domains. *Math. Meth. Appl. Sci.*, 21:823–864, 1998.

[2] F. Armero and J.C. Simo. Long-term dissipativity of time-stepping algorithms for an abstract evolution equation with applications to the incompressible MHD and Navier-Stokes equations. *Comput. Methods Appl. Mech. Engrg.*, 131:41–90, 1996.

[3] D.N. Arnold, F. Brezzi, B. Cockburn, and L.D. Marini. Unified analysis of discontinuous Galerkin methods for elliptic problems. *SIAM J. Numer. Anal.*, 39:1749–1779, 2001.

[4] R. Berton. *Magnétohydrodynamique*. Masson, 1991.

[5] S.C. Brenner. Poincaré-Friedrichs inequalities for piecewise H^1-functions. *SIAM J. Numer. Anal.*, 41:306–324, 2003.

[6] F. Brezzi and M. Fortin. Mixed and hybrid finite element methods. In *Springer Series in Computational Mathematics*, volume 15. Springer–Verlag, New York, 1991.

[7] F. Brezzi and M. Fortin. A minimal stabilisation procedure for mixed finite element methods. *Numer. Math.*, 89:457–491, 2001.

[8] B. Cockburn, G. Kanschat, and D. Schötzau. Local discontinuous Galerkin methods for the Oseen equations. *Math. Comp.*, 73:569–593, 2004.

[9] B. Cockburn, G. Kanschat, and D. Schötzau. A locally conservative LDG method for the incompressible Navier-Stokes equations. *Math. Comp.*, 74:1067–1095, 2005.

[10] B. Cockburn, G. Kanschat, and D. Schötzau. A note on discontinuous Galerkin divergence-free solutions of the Navier-Stokes equations. *J. Sci. Comp.*, 31:61–73, 2007.

[11] B. Cockburn, G.E. Karniadakis, and C.-W. Shu, editors. *Discontinuous Galerkin Methods. Theory, Computation and Applications*, volume 11 of *Lect. Notes Comput. Sci. Eng.* Springer–Verlag, 2000.

[12] B. Cockburn and C.-W. Shu. Runge–Kutta discontinuous Galerkin methods for convection–dominated problems. *J. Sci. Comp.*, 16:173–261, 2001.

[13] B. Cockburn and C.-W. Shu. Foreword for the special issue on discontinuous Galerkin methods. *J. Sci. Comp.*, 22:1–3, 2005.

[14] M. Costabel and M. Dauge. Weighted regularization of Maxwell equations in polyhedral domains. *Numer. Math.*, 93:239–277, 2002.

[15] T. G. Cowling. *Magnetohydrodynamics*. Adam Hilger, England, 1976.

[16] M. Dauge. Stationary Stokes and Navier–Stokes systems on two- or three-dimensional domains with corners. Part I: Linearized equations. *SIAM J. Math. Anal.*, 20:74–97, 1989.

[17] C. Dawson. Foreword for the special issue on discontinuous Galerkin methods. *Comput. Methods Appl. Mech. Engrg.*, 195:3, 2006.

[18] J.-F. Gerbeau. *Problèmes mathématiques et numériques posés par la modélisation de l'électrolyse de l'aluminium.* PhD thesis, Ecole Nationale des Ponts et Chaussées, 1998.

[19] J.-F. Gerbeau. A stabilized finite element method for the incompressible magnetohydrodynamic equations. *Numer. Math.*, 87:83–111, 2000.

[20] J.-F. Gerbeau, C. Le Bris, and T. Lelièvre. *Mathematical methods for the magnetohydrodynamics of liquid metals*. Numerical mathematics and scientific computation. Oxford University Press, New York, 2006.

[21] V. Girault and P.A. Raviart. *Finite element methods for Navier–Stokes equations*, volume 5 of *Springer Series in Computational Mathematics*. Springer–Verlag, New York, 1986.

[22] J.-L. Guermond and P. Minev. Mixed finite element approximation of an MHD problem involving conducting and insulating regions: the 3D case. *Num. Meth. Part. Diff. Eqs.*, 19:709–731, 2003.

[23] M.D. Gunzburger, A.J. Meir, and J.S. Peterson. On the existence and uniqueness and finite element approximation of solutions of the equations of stationary incompressible magnetohydrodynamics. *Math. Comp.*, 56:523–563, 1991.

[24] P. Hansbo and M.G. Larson. Discontinuous Galerkin methods for incompressible and nearly incompressible elasticity by Nitsche's method. *Comput. Methods Appl. Mech. Engrg.*, 191:1895–1908, 2002.

[25] J.S. Hesthaven and T. Warburton. *Nodal Discontinuous Galerkin Methods: Algorithms, Analysis, and Applications*, volume 54 of *Texts in Applied Mathematics*. Springer, 2008.

[26] R. Hiptmair. Finite elements in computational electromagnetism. *Acta Numerica*, 11:237–339, 2002.

[27] P. Houston, I. Perugia, and D. Schötzau. Mixed discontinuous Galerkin approximation of the Maxwell operator. *SIAM J. Numer. Anal.*, 42:434–459, 2004.

[28] P. Houston, I. Perugia, and D. Schötzau. Mixed discontinuous Galerkin approximation of the Maxwell operator: Non-stabilized formulation. *J. Sci. Comp.*, 22:315–346, 2005.

[29] P. Houston, I. Perugia, and D. Schötzau. Mixed discontinuous Galerkin approximation of the Maxwell operator: The indefinite case. *Math. Model. Numer. Anal.*, 39:727–754, 2005.

[30] C. Johnson and J. Pitkäranta. An analysis of the discontinuous Galerkin method for a scalar hyperbolic equation. *Math. Comp.*, 46:1–26, 1986.

[31] F. Li and C.-W. Shu. Locally divergence-free discontinuous Galerkin methods for MHD equations. *J. Sci. Comp.*, 22–23:413–442, 2005.

[32] P. Monk. *Finite element methods for Maxwell's equations*. Oxford University Press, New York, 2003.

[33] J. C. Nédélec. Mixed finite element in $\mathbb{R}^3$. *Numer. Math.*, 50:57–81, 1980.

[34] I. Perugia and D. Schötzau. The *hp*-local discontinuous Galerkin method for low-frequency time-harmonic Maxwell's equations. *Math. Comp.*, 72:1179–1214, 2001.

[35] D. Schötzau. Mixed finite element methods for incompressible magneto-hydrodynamics. *Numer. Math.*, 96:771–800, 2004.

[36] D. Schötzau, C. Schwab, and A. Toselli. Mixed *hp*-DGFEM for incompressible flows. *SIAM J. Numer. Anal.*, 40:2171–2194, 2003.

[37] T.C. Warburton and G.E. Karniadakis. A discontinuous Galerkin method for the viscous MHD equations. *J. Comput. Phys.*, 152:608–641, 1999.